NASA
Technical
Paper
2380

December 1984

Full-Scale Crash-Test Evaluation of Two Load-Limiting Subfloors for General Aviation Airframes

Huey D. Carden

NASA

NASA Technical Paper 2380

1984

Full-Scale Crash-Test Evaluation of Two Load-Limiting Subfloors for General Aviation Airframes

Huey D. Carden

Langley Research Center
Hampton, Virginia

National Aeronautics and Space Administration

Scientific and Technical Information Branch

Contents

Summary

Three general aviation airplane test specimens were crash tested at the Langley Impact Dynamics Research Facility under controlled free-flight conditions. The airplanes were six-place, low-wing airplanes with twin engines. One structurally unmodified airplane was the base-line specimen for the test series. The other two airplanes were structurally modified to incorporate load-limiting (energy-absorbing) subfloor concepts into the structure for full-scale crash test evaluation and for comparison with the unmodified-airplane test results.

Typically, the lowest floor accelerations, the lowest anthropomorphic-dummy responses, and the least seat crushing of standard and load-limiting seats occurred in the airplanes modified with load-limiting subfloors, wherein the greatest structural crushing of the subfloor took place. The better performing of the two load-limiting subfloor concepts reduced the peak airplane floor accelerations to $-25g$ to $-30g$ as compared with approximately $-40g$ to $-55g$ for the unmodified airplane structure.

The structural crushing of the load-limiting subfloors also minimized the upward heave of the cabin floor into the liveable cabin volume (i.e., a volume sufficient to maintain space between occupants and the cabin structure). However, the nonsymmetric heave of the floor caused operational problems with a vertical-stroking load-limiting seat and highlights the necessity for such seats to be able to accommodate nonsymmetric floor behavior but still function properly.

Introduction

Since 1973, NASA has investigated the crash dynamics of general aviation airplanes under controlled free-flight impact conditions. The objectives of this program were to determine the dynamic response of airplane structures, seats, and occupants during a crash, and to determine the effect of flight parameters at impact on loads and on structural damage. NASA has conducted 32 controlled, full-scale crash tests of general aviation airplanes and has generated a substantial data base on crash behavior (refs. 1 to 12). Within the crash dynamics program, a specific area of research involved the development of structural concepts to limit the load transmitted to the occupants of an airplane (ref. 8). The objective of this phase of the crash dynamics research was to control the load transmitted by a structure to the airplane occupants either by modifying the structural arrangement or by adding specific load-limiting devices to help dissipate the kinetic energy. The research on load-limiting concepts applicable to metal airframe structures of general aviation aircraft consisted of the following three phases:

1. Development of concepts
2. Design, fabrication, and testing of full-scale floor sections
3. Modification of full-scale aircraft structures

In the first phase, several structural concepts of energy-absorbing lower fuselage structures were developed, and tests were conducted to determine the performance of the structures. The five most promising concepts were then selected for the design of full-scale floor sections. (See ref. 13.)

In the second phase, full-scale floor sections were designed that featured a high-strength structural platform supported by a crushable subfloor structure. The platform provided structural integrity for the attachment of standard or energy-absorbing seats. The subfloor structure made use of the crashworthy concepts to provide a "crush zone" for crash-impact energy absorption and load control. Following the design effort, 18 floor sections (3 or 4 sections for each of the 5 concepts) were fabricated. Static tests were then conducted to determine the load-deflection characteristics for each concept, and dynamic drop tests were made to determine the crash-impact response of the floor sections. (See refs. 8, 13, and 14.) After evaluation of the floor test results based primarily on performance and energy absorbed per unit weight, two concepts were selected for incorporation into a full-scale fuselage design.

In phase three, two twin-engine-airplane fuselages were modified by incorporating floor sections (see ref. 14) which were to be tested along with standard and load-limiting seat-dummy combinations for comparison with test results from an unmodified fuselage. The purpose of this report is to present a comparison of the results of the full-scale test evaluation of the two crashworthy structure concepts with the unmodified fuselage used in the investigation.

Test Facility and Procedures

Facility

The crash tests were performed at the Langley Impact Dynamics Research Facility (shown in fig. 1). The gantry is composed of truss elements arranged with three sets of inclined legs to give vertical and lateral support and another set of inclined legs to provide longitudinal support. The gantry is 73 m high and 122 m long. The supporting legs are spread 81 m apart at the ground and 20 m apart at the 66-m level. An enclosed elevator and a stairway provide access to the overhead work platforms, and catwalks permit safe traverse of the upper levels of the gantry. A movable bridge spans the gantry at the 66-m level and traverses the length of the gantry. Shown in figure 2 is a sketch of a full-scale airplane specimen suspended from the gantry in the position ready to be swung onto the impact surface. The

reinforced concrete impact surface permits tests to be repeated and allows comparison between tests. Detailed information about the facilities used to carry out a successful aircraft crash test is reported in reference 15.

Crash-Test Technique

The test technique used to crash the airplane specimens is shown schematically in figure 3. The airplane specimen, suspended by two swing cables attached to the top of the gantry, is drawn back to a height of about 49 m above the impact surface by a pullback cable. The test sequence begins when the airplane specimen is released from the pullback cable. The specimen swings pendulum style onto the impact surface. For the series of tests reported herein, a velocity augmentation system (VAS) was used to attain the desired higher flight-path velocity. Four solid-propellant rockets were mounted symmetrically on the engine nacelles to provide additional thrust (up to 77 800 N). The airplane is released after rocket ignition, and the rockets continue to burn during most of the downward acceleration trajectory but are at zero thrust at impact. The number and burn time of the rockets determines the velocity achieved with the VAS test method. The swing cables are pyrotechnically separated from the airplane specimen when it is about 1 m above the impact surface to free it from restraint during the crash impact. The umbilical cable remains attached during the impact for data acquisition and is pyrotechnically separated about 0.75 sec after swing-cable separation.

Airplane Suspension System

The airplane suspension system used to control the swing and impact attitude of this airplane specimen is shown in figure 4. The swing and pullback cables connect to the swing and pullback harnesses. The swing harness consists of two swing-cable extensions which attach to the wing hard points to support the airplane specimen and to control roll angle. There are two sets of pitch cables that connect to the swing-cable rings and to the fuselage hard points fore and aft of the airplane center of gravity to control the angle of attack. The interaction of all cables in the harness system is involved in yaw control. The pullback harness consists of a pair of cables attached to the wing hard points and a bar which spreads the cables to clear the airplane fuselage and empennage. The pullback cable attached to this harness is used to pull the airplane to the height necessary to produce (with the assistance of the solid propellant rockets) the desired velocity at impact. An umbilical cable links the onboard instrumentation to a data-acquisition system located in a building adjacent to the gantry.

Test Parameters

The flight-path angles and attitude angles for the airplanes are identified in figure 5, along with the reference axes. Positive force directions coincide with the reference axes. The actual test parameters for the tests reported herein, along with a photograph illustrating the impact attitude for each airplane test specimen, are presented in figure 6. For consistency and brevity, each test and each airplane specimen is hereafter identified by word descriptions (i.e., unmodified, corrugated-beam–notched-corner and notched-corner structures) for impact parameters presented in figure 6. The nominal flight-path velocity was 36.8 m/sec, which is approximately the stall speed for an airplane of this type. The test conditions were chosen to provide nominally zero yaw and roll and approximately a 9.1 m/sec vertical velocity component which was the design goal capability for the subfloors.

Airplane Test Specimens

Airplane specimens used for the tests were twin-engine, low-wing, general aviation airplanes with a pressurized cabin having a nominal mass of 3400 kg with a capacity of six occupants. The airplane specimens were structurally complete except for the upholstery and avionics. Engines were simulated masses with proper inertia and center-of-gravity locations. A reduced-size flat-plate stabilizer-elevator combination was used on the tail. Water was put into the fuel tanks to simulate the fuel mass. In addition, inflated rubber inner tubes were used in the fuel tanks to take up the remaining air volume and to minimize sloshing. Spoilers were attached to the wings to minimize the aerodynamic lift. The landing gear was in the retracted position for the crash tests. The exterior and interior of the airplane specimens were painted to enhance the photographic contrast, and black lines were painted over rivet lines to delineate the underlying structure.

Structural modifications. On two of the airplanes, the fuselage subfloor structure from the main wing spar at fuselage station (FS) 3.56 m to aft of the rear cabin door at FS 6.20 m was replaced with a crashworthy subfloor structure. The modified area is illustrated in figure 7. Of the existing structures, the upper floor panel was not modified, but the keel beams, bulkheads, stringers, and lower contour skin were removed and the corrugated-beam–notched-corner or notched-corner structures (see ref. 14) were installed. Modification of the airplane with the notched-corner design increased the original airplane weight by approximately 6.8 kg whereas the corrugated-beam–notched-corner design increased the weight by approximately 9.1 kg. For a 2724-kg airplane, the weight increases were

0.25 percent of gross weight for the notched-corner design and 0.33 percent of gross weight for the corrugated-beam–notched-corner design. Original design of load-limiting concepts into an airplane structure rather than retrofitting them as discussed herein would probably result in no weight penalty. The crashworthy subfloor structure was designed to maintain lower fuselage contour, including the skin gauge. Standard but higher strength seat tracks capable of sustaining a single-point vertical load of 20 000 N were installed on the upper floor panel to provide seat attachment capability. Figures 8 and 9 illustrate details of the construction of the corrugated-beam–notched-corner and the notched-corner subfloor structures, respectively. Further details of the modifications are given in reference 14.

Standard and load-limiting seats. The three airplanes used the seating and passenger arrangements shown in figure 10. Anthropomorphic dummies, each with a mass of 75 kg (all 50th percentile (ref. 16)), occupied the seats except for the copilot position, for which there was no seat. The first and third passenger seats were standard equipment for an airplane of this type and were equipped with a lap belt only. (See fig. 11(a).) A minor modification of replacing the rubber diaphragm seat pan with an aluminum pan riveted to the seat frame (to prevent the cushion from being punched through) was made to all the standard seats. The pilot, second passenger, and fourth passenger seats were three different types of load-limiting seats. The pilot seat was a prototype of an energy-absorbing seat supplied by a private organization. The front legs of the seat were S-shaped legs for energy absorption by bending, and the rear legs (see fig. 11(b)) were slanted rearward to also provide energy absorption by bending. The second passenger seat was an experimental version of an energy-absorbing seat designed for use in helicopters. A composite tube which crushes at a prescribed load is the load-limiting mechanism in the seat. The seat bucket (see fig. 11(d)) traverses down two vertical guides as the composite tube crushes. The fourth passenger seat (see fig. 11(c)) uses a wire-bending mechanism as a load-limiting device. In this seat the wire-bending mechanism is housed in the two diagonal legs. The diagonal legs with the wire-bending (load-limiting) mechanism move upward into the seat back as the seat pivots forward and downward on the four-bar linkage leg arrangement. Reference 9 gives more complete details on this seat arrangement and operation.

Figure 10 illustrates the arrangement of the occupants and restraints for each test, and the restraints are also visible in figure 11. All lap belts and shoulder harnesses (except for the pilot's) were secured to the seats. The pilot was restrained with a lap belt attached to the seat and with a double shoulder harness attached to the fuselage. The restraint system assembly strength was at least 6672 N as required by the FAA regulations.

Instrumentation and Data Preparation

Onboard instrumentation for obtaining data pertaining to the dynamic behavior of the airplane structure, the seats, and the dummies consisted of dc accelerometers (piezo-resistive) and high-speed motion-picture cameras. (See figs. 2 and 12.) External motion-picture coverage of the crash sequence at various film speeds was provided by tracking and fixed cameras located to the port side, front, back, and overhead of the airplane test specimen. A Doppler radar unit was used to obtain the horizontal velocity of the test specimen at impact.

The locations and orientation (i.e., normal, longitudinal, and transverse) of the accelerometers onboard the airplanes are shown in figure 12(a), and the locations and orientation of the accelerometers in the dummies are shown in figure 12(b). Each accelerometer is designated by its grid coordinates as follows: the first number indicates the longitudinal coordinate; the first letter indicates the normal coordinate (floor to roof); the second number indicates the transverse coordinate; and the second letter indicates the accelerometer orientation with respect to the airplane body-axis system. The normal, longitudinal, and transverse orientations are designated as N, L, and T. For example, the normal accelerometer location in the center of the ceiling of the cockpit is designated 11I4N. This system applies to the identification of all structural accelerations.

The physical variables measured in the aircraft specimen were converted to electrical signals by the transducers. The transducers were wired to a 90-channel data chassis in groups of 5 channels through a high-speed electronic switch with a regulated 10-V power supply common to all channels. This arrangement prevents dead shorts in a channel in any group from adversely affecting other data channels. From the data chassis in the airplane, the signals were transmitted through an umbilical cable to a junction box on top of the gantry. From there they were transmitted through hard wire to the control room. In the control room, the signals were received through another junction box and sent to a patchboard that has a 150-channel capability. From the patchboard, the signals were fed to the signal-conditioning units, where they were filtered through a 600-Hz low-pass filter and amplified. The signals were multiplexed by a 90-channel multiplex FM system, which incorporates five frequencies: 25, 40, 55, 70, and 85 kHz. The signals were then recorded directly onto magnetic tape by a 28-track recorder. The first 18 tracks were dedicated for the 90 data channels (5 channels per track). Tracks 27 and 28 were reserved for voice annotation and time code, respectively. The

data on the magnetic tapes were digitized at 4000 samples per second and filtered as follows:

Dummy head, Hz	600 (unfiltered)
Dummy chest, Hz	180
Dummy pelvis, Hz	180
Floor structure, Hz	20

The data were utilized to produce computer-generated histories of the accelerations or of other measured parameters. Some plots on the figures are blank because the data were lost as the result of physical and electrical instrumentation failures.

Results and Discussion

Crash Dynamics

Figure 13 presents a series of photographs illustrating the crash sequence typical of the three tests in the investigation of load-limiting structural concepts. The sequence, from top to bottom in rows left to right at unspecified time intervals, begins shortly after release of the airplane from the pullback position. The rocket plumes are readily visible in the photographs. The last five photographs in the sequence show the airplane approaching the impact surface in the flat, or belly-landing, attitude used to test the load-limiting subfloors. Areas damaged during the crash are not readily observable in the sequences because the major structural damage was confined to the underside of the airplane for the $-15°$ flight path and the $0°$ pitch impact attitude.

Figure 14 shows the damaged underside of two of the three airplanes. The broken engine mounts and dangling engines are typical of the damage. The interior photographs of figure 15 show the relative differences between the unmodified subfloor, the corrugated-beam–notched-corner subfloor, and the notched-corner subfloor structures. Readily visible in the figure is the heaved-up floor of the unmodified structure with little subfloor crushing compared with the relatively level floors of the corrugated-beam–notched-corner and notched-corner structures. Considerable crushing of the subfloors is apparent in the modified airplanes. The influence of the floors remaining level but the subfloors crushing is discussed in the following sections. Throughout the crash sequence, the liveable cabin volume was maintained in each of the three airplane specimens, liveable volume being a volume sufficient to maintain space between the occupants and the cabin structure.

Floor Behavior

Crash pulses. The normal and longitudinal crash pulses of the airplane structure for the three test specimens are presented in figures 16 to 21. The three rows of plots in each figure (except fig. 17) present the crash pulse data for the outboard track forward, the inboard track forward, and the inboard track aft for the unmodified, corrugated-beam–notched-corner, and notched-corner airplanes. The data are presented in this format for the pilot and copilot positions and for the first to the fourth passenger positions in the airplane. Figure 22 presents similar data for the airplane tail cone and for the emergency locator transmitter (ELT) unit, and figure 23 presents data for the cockpit roof, the center roof, and the rear roof locations.

The data in figures 16 to 23 indicate the accelerations decreased in severity in the following order of structures: the unmodified structure, the notched-corner structure, and the corrugated-beam–notched-corner structure. The peak normal accelerations for the unmodified airplane were between $-40g$ and $-55g$ over the length of the airplane. In comparison, the peak normal accelerations for the notched-corner structure, which allowed some crushing of the subfloor structure, were generally $-35g$ to $-45g$, and the peak normal accelerations for the corrugated-beam–notched-corner structure, which allowed the most subfloor structural crushing, were reduced to the lowest values of approximately $-25g$ to $-30g$, or about 50 percent of the peak normal accelerations of the unmodified airplane.

For the roof line normal accelerations in figure 23, the flexibility of the fuselage barrel between the floor and the upper crown also increased the severity of the normal accelerations relative to the accelerations experienced at the floor level.

Figure 24 is a summary bar graph comparing the average peak normal crash pulses for the cockpit, the center cabin, and the rear cabin areas for the three test airplanes. The graph shows, as previously indicated, that the two airplanes with modified subfloor structures substantially reduced the acceleration loads in the airplane below those experienced in the unmodified airplane.

The peak longitudinal accelerations in the airplanes were between $-7.5g$ to $-12.5g$ for all fuselage locations except for the ELT unit. The higher longitudinal accelerations for the ELT unit in the tail-cone structure (see fig. 22(b)) resulted because of amplification of the input by the flexibility of the mounting structure for the unit.

Structural crushing. A comparison of the structural crushing that occurred in the three test airplanes is presented in figure 25. The amount of crushing at a common cross section of the airplanes is inversely proportional to the peak acceleration levels experienced for the floor structure. For example, a minimum amount of crushing occurred in the unmodified airplane, and the correspondingly large heave distance is indicative of the high loads transmitted directly from the outer

skin to the floor surface in this test. In contrast, the large amount of structural crushing and minimum heave distance noted in the corrugated-beam–notched-corner structure are indicative of the much lower loads that were produced in the modified structures. The crushing of the subfloor structure occurred, by design, at lower loads, thus limiting the transmitted forces. The upward heave of the floor was the only encroachment of structure into the liveable cabin volume that occurred for the three test airplanes. The magnitude of the accelerations and the structural response behavior noted in the full-scale test airplanes (both modified and unmodified) are quite similar to the magnitudes and behavior observed for the subfloor sections discussed in references 8, 13, and 14.

Seat Behavior

Photographs of the standard and load-limiting seats showing the deformations caused by the loads of the floor structure and the occupants for each of the airplanes are presented in figure 26.

Standard seats. Figure 26(a) shows three standard passenger seats, one from each of the three test airplanes. The seats are arranged in order of most damaged to least damaged from left to right. The seat at the left in figure 26(a) was from the unmodified airplane and sustained the highest loads; as shown, it also sustained the most damage. The understructure supports of the seats were crushed and the rear cross member was severely bent as the cushion was punched through by the dummy occupant.

The center picture in figure 26(a) is the seat taken from the notched-corner-subfloor airplane. This seat sustained less damage than the seat in the unmodified-subfloor airplane because the moderate subfloor crushing produced lower loads in the seat. The understructure of this seat is just beginning to show signs of crushing under the $-30g$ to $-40g$ loads produced at the floor level. This also confirms earlier static test results (ref. 9) that indicate this type of seat crushes above $-30g$, a g-loading which is too high for human tolerance. (See ref. 17.) Because the crushing of the standard seats involved considerable distortion, buckling, tearing, and breakup of the seat structure, no attempt was made to report the amount of crushing for these seats.

The third seat at the right in figure 26(a) was taken from the airplane with the corrugated-beam–notched-corner subfloor and shows only minor seat cushion compression and no structural damage. This also indicates that the lowest seat loads were developed through the crushable subfloor in this airplane.

Load-limiting seats. Figure 26(b) shows stroked configurations of the three different load-limiting seats illustrating typical behavior of the seats during all three crash tests. Table I presents measured strokes for the three seats. The left seat in figure 26(b) (with the S-shaped legs) was in the pilot position, which was not over the modified subfloor structure. The behavior of this seat involved plastic deformations of the front S-leg and bending of the rear legs. Additionally, breaks occurred in the rear legs at the floor-attachment point and at the weld location on the bottom of the front S-leg. As indicated in a previous section, the pilot dummy in this seat had a lap-belt–shoulder-harness arrangement, with the belt attached to the seat and the shoulder harness attached to the roof structure. With the crushing of the seat, the harness tended to pull up on the seat belt causing undesirable restraint and allowing potential submarining of the occupant. As shown in table I, the maximum strokes for the seat in the three crash tests followed the same trend as did the maximum floor accelerations noted in the section entitled "Crash Pulses." For instance, the S-leg seat in the unmodified-structure airplane underwent the largest stroke (14.2 cm), the seat in the notched-corner airplane incurred the next largest stroke (10.7 cm), and the seat in the corrugated-beam–notched-corner airplane sustained the smallest stroke (9.9 cm).

The seat shown in the center of figure 26(b) is an experimental version of a load-limiting seat designed for helicopter applications. The seat was used in the present series of crash tests to evaluate a seat which allows only vertical stroking. The full stroke capability of this seat (15.2 cm) was used in all three tests. In fact, the seat bottomed out in the unmodified airplane. A number of factors in the behavior of the seat during the crash tests led to the use of the entire stroke. The primary factor was the uneven, upward heaving of the floor during the crash. This introduced undesirable bending and misalignment into the load-limiting mechanism. The misalignment of the plunger caused eccentric loads on the composite energy-absorbing tube. The eccentric loads crushed only one side of the composite tube (see fig. 27), leading to an excessive stroke at reduced stroking force. (Design improvements have been introduced into this seat type to eliminate a number of operational difficulties.)

The third seat, at the right in figure 26(b), is the wire-bending load-limiting seat. The configuration shown was typical for the three crash tests. During the crash tests, the load-limiting mechanism worked as designed and a portion of the diagonal load-limiter stroked upward into the back region of the seat. An assessment of the inboard and outboard load-limiter strokes in table I indicates the heaving up of the floor surface introduced nonsymmetric stroking, but the seat accommodated this nonsymmetry and functioned properly. For example, in the unmodified-airplane test, the inboard

stroke was approximately 4.1 cm greater than the outboard stroke, whereas for the test with the corrugated-beam–notched-corner airplane, the strokes were approximately 50 percent less than the strokes for the unmodified structure and the inboard stroke was only 1.9 cm greater than the outboard stroke. The smaller difference between the two strokes is directly attributable to the behavior of the floor. For instance, the corrugated beams collapsed more evenly and thus distributed more uniform and lower loads to the upper floor, resulting in only minor upward heave of the floor.

Anthropomorphic-Dummy Responses

The resultant accelerations that occurred in the head, chest, and pelvis of the anthropomorphic dummies during the various crash tests are presented in figure 28. Individual responses of the dummies in the normal, longitudinal, and transverse directions are presented in the appendix.

Standard seats. The first and third passenger dummies were seated in standard seats. A comparison of the responses in these dummies for the three test airplanes indicated a trend in the resultant accelerations in their head, chest, and pelvis that was generally consistent with and similar to trends (but to a less obvious degree) discussed for the structural crushing and the floor accelerations in the sections entitled "Crash Pulses" and "Seat Behavior." Although specific dummy responses may have varied from the previous trends from test to test, the overall behavior is still considered to be similar; that is, the highest dummy response peaks occurred for the tests of the unmodified structure, the lowest peaks occurred for the tests of the corrugated-beam–notched-corner structure, and the notched-corner structure produced dummy peak responses between these two cases. In addition, a comparison of the dummy accelerations with the corresponding accelerations of the floor structure indicates that the seat-occupant system did not amplify the input from the floor in these tests.

A comparison of the shapes of the dummy response histories indicates that the corrugated-beam–notched-corner structural crushing altered the character of the response compared with the results for the unmodified and notched-corner airplanes. The dummy response in the latter two tests had high initial peaks, whereas the response for the corrugated-beam–notched-corner structure was smoother and lower in magnitude. Sharp, high acceleration spikes of the resultant head responses for the first passenger in the notched-corner test and for the third passenger in the corrugated-beam–notched-corner test were the result of head contact with the seat back in the case of the first passenger and with the roof structure in the case of the third passenger. The spikes were verified as being from these causes from an analysis of interior motion-picture film coverage of the tests. An assessment of the film indicated that, although considerable pain would have been experienced from these secondary impacts, the blows would not have been fatal, and certainly the blows would have been alleviated somewhat if the upholstery (removed for all tests) had been in place.

It may be noted that the occupant responses of the first and third passengers generally reflected the reduction of loads produced by the subfloor modifications. That is, the lowest occupant responses were generally for the corrugated-beam–notched-corner structure, which also produced the lowest floor responses. This illustrates the concept of using the subfloor as one of several potential load-limiting zones for controlling the crash environment, as discussed in reference 8.

Load-limiting seats. The pilot and the second and fourth passenger locations contained the load-limiting seats. Results for these dummy occupants in figure 28 indicate that the fourth passenger response was the least severe, followed in turn by the pilot and the second passenger. The shapes of the responses for the second passenger were different compared with the other occupant response shapes in all three test airplanes. The peak response for the second passenger occurred later in the acceleration pulse primarily because of the bottoming out of the stroke mechanism, as discussed previously. Generally, the best occupant response occurred for the corrugated-beam–notched-corner airplane, with the least desirable responses occurring in the unmodified structure test. An important observation should also be made for the pilot response in the S-leg load-limiting seat. This seat was on the unmodified floor structure, but the resultant occupant responses for all three tests were quite similar since the crushing of the seat is controlling the occupant response. The reduced loads produced by the subfloor modifications were not reflected in the occupant responses but were reflected in the seat strokes. (See table I.) These responses for the pilot also illustrate the use of a load-limiting seat rather than a subfloor structure as the energy-absorbing or load-limiting zone, a concept which is also discussed in reference 8.

The resultant head response of the fourth passenger exhibited a short-duration, high-amplitude acceleration spike for the corrugated-beam–notched-corner test which was also confirmed by interior motion-picture film coverage to be a secondary head impact on the airplane roof structure. The blow most probably would not have been fatal but would have been very painful to an occupant. As was noted for the responses of the dummies in the standard seat, no undesirable amplification of the floor inputs at the seat base occurred in

the dummies for the three load-limiting seat-occupant systems in these tests.

Concluding Remarks

Three six-place, low-wing, twin-engine general aviation airplanes were crash tested at the Langley Impact Dynamics Research Facility under controlled free-flight conditions. One structurally unmodified airplane was the base-line specimen for the test series. The other two airplanes were structurally modified to incorporate load-limiting (energy-absorbing) subfloor concepts into the structure for full-scale crash-test evaluation and for comparison with the unmodified-airplane test results. All airplanes were impacted on a concrete surface at a nominal flight-path velocity of 37 m/sec, a flight-path angle of $-15°$, and a pitch angle of 0° (flat impact).

The normal and longitudinal acceleration histories (crash pulses) in the airplanes at five anthropomorphic-dummy locations and on the airplane roof and tail-cone locations are presented for each crash test. Typically, the peaks of the crash pulse for a given test were essentially the same from the nose to the tail of the airplanes because of the flat impact.

The lowest floor accelerations and the least seat crushing occurred in the modified (load-limiting subfloor) airplanes in which the greatest structural crushing of the subfloor took place. The better performing of the two load-limiting subfloors, the corrugated-beam–notched-corner subfloor, reduced the floor peak accelerations at the pilot and at four seat-occupant locations to $-25g$ to $-30g$ compared with approximately $-40g$ to $-55g$ for the unmodified airplane. The structural crushing of the load-limiting subfloors also minimized the upward heave of the cabin floor, which in the unmodified airplane was the only intrusion into the liveable cabin volume (i.e., a volume sufficient to maintain space between occupants and the cabin structure). Liveable cabin volume was maintained in all three crash-test airplanes. The upward heave of the floor caused operational problems with a vertical-stroking load-limiting seat and highlights the necessity for such seats to be able to accommodate nonsymmetric floor behavior but still function properly.

Occupant acceleration responses generally reflected the same trends as the structural accelerations; that is, the lower responses occurred for the modified subfloor airplanes. Furthermore, the pilot responses (on an unmodified structure even in the modified-subfloor airplanes) illustrated the use of a load-limiting seat to create the controlling (load-limiting) crush zone. On the other hand, the responses of the first and third passengers in standard seats on the modified structures reflect the use of the airplane subfloor as the controlling crush zone.

Langley Research Center
National Aeronautics and Space Administration
Hampton, Virginia 23665
September 24, 1984

Appendix

Anthropomorphic-Dummy Responses

This appendix presents the individual acceleration histories of the anthropomorphic dummies used in the three crash tests. Normal, longitudinal, and transverse accelerations in the head and normal and longitudinal accelerations in the pelvis and chest of each dummy are included in figures A1 to A3. The resultant accelerations, presented in the main text under the section entitled "Anthropomorphic-Dummy Responses," are derived from the data of figures A1 to A3. The pertinent comments about the data included in the main text apply basically to the individual responses presented in figures A1 to A3 and are therefore not repeated here.

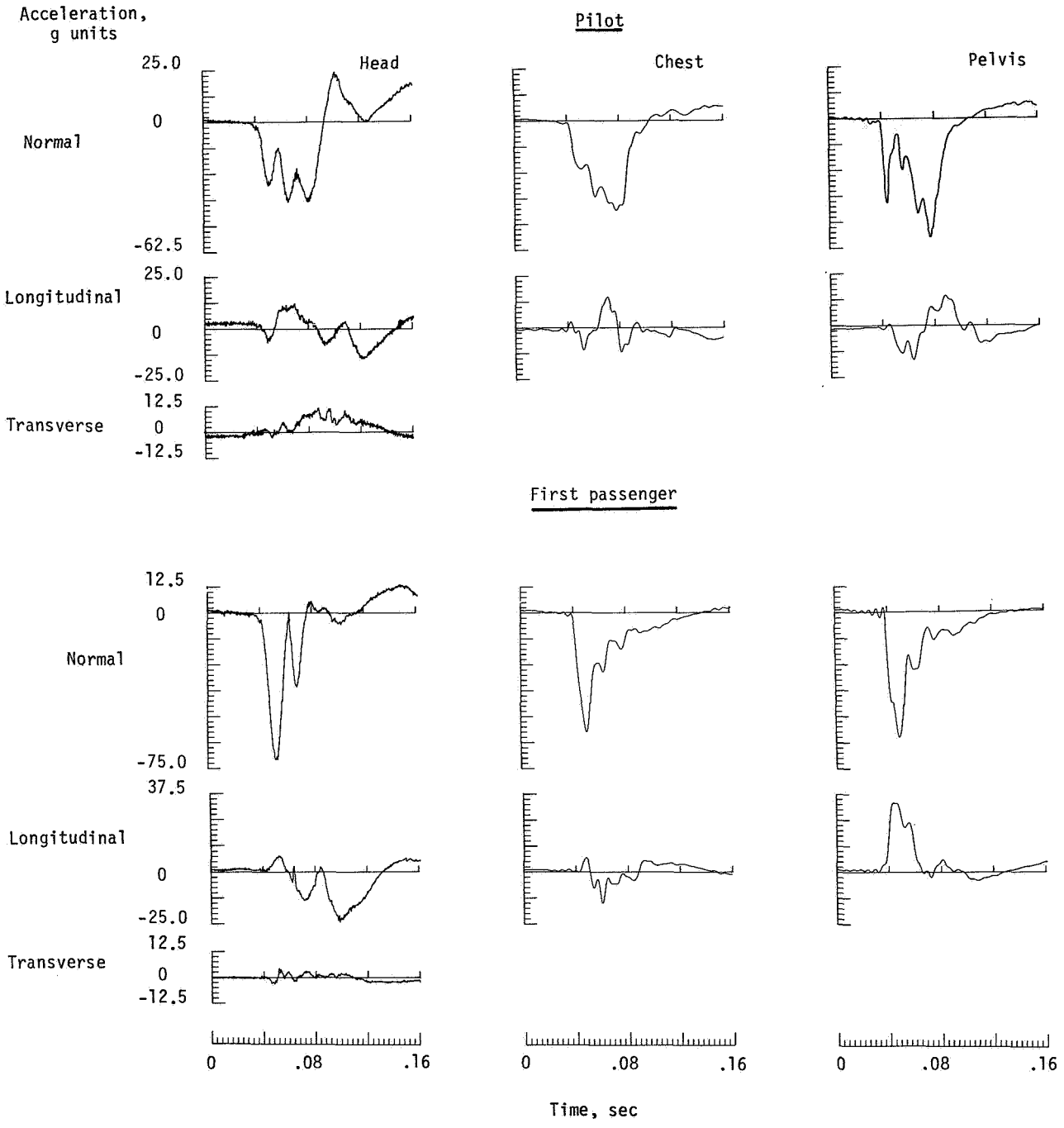

(a) Pilot and first passenger.

Figure A1. Accelerations in anthropomorphic-dummy occupants for unmodified airplane.

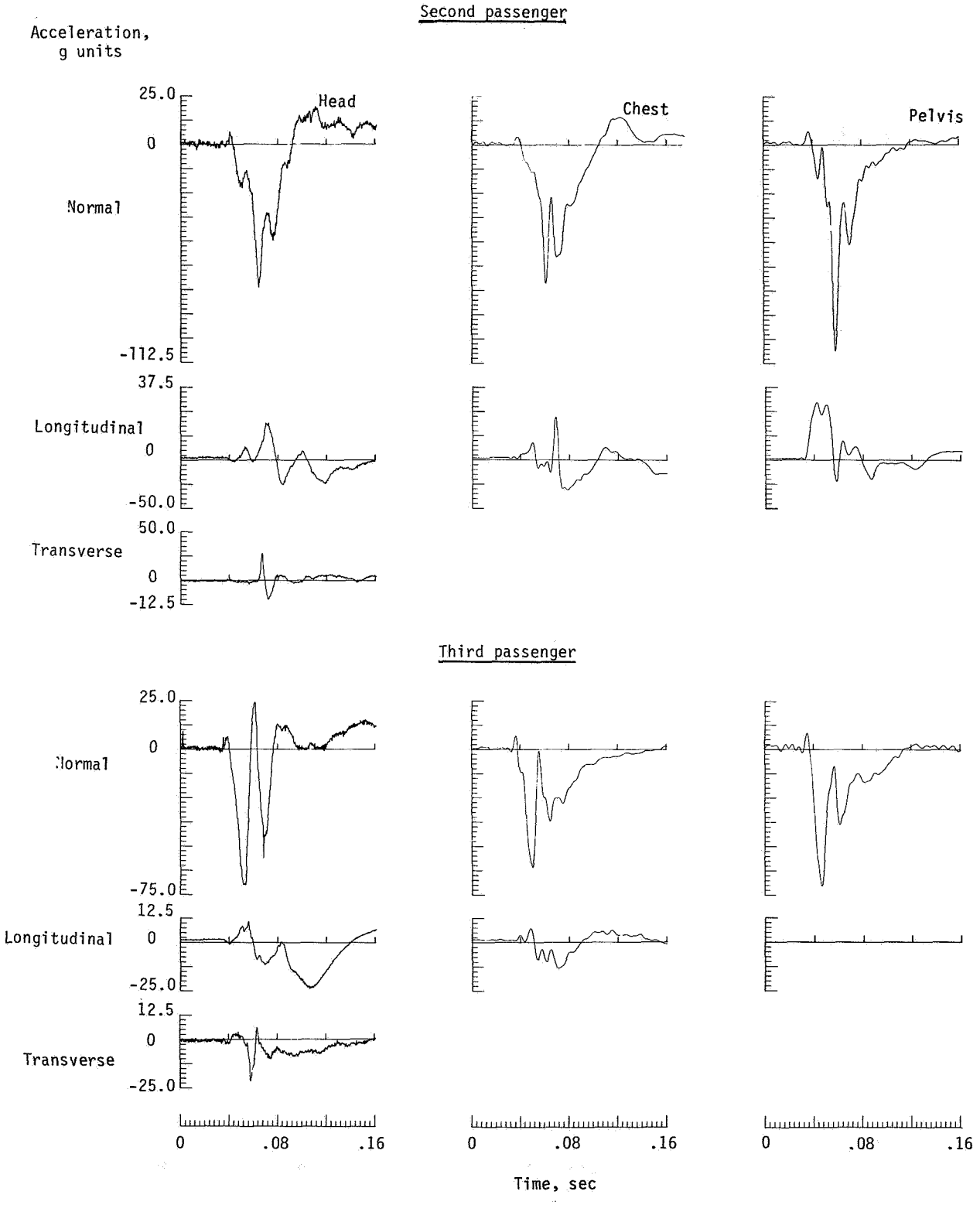

(b) Second and third passengers.

Figure A1. Continued.

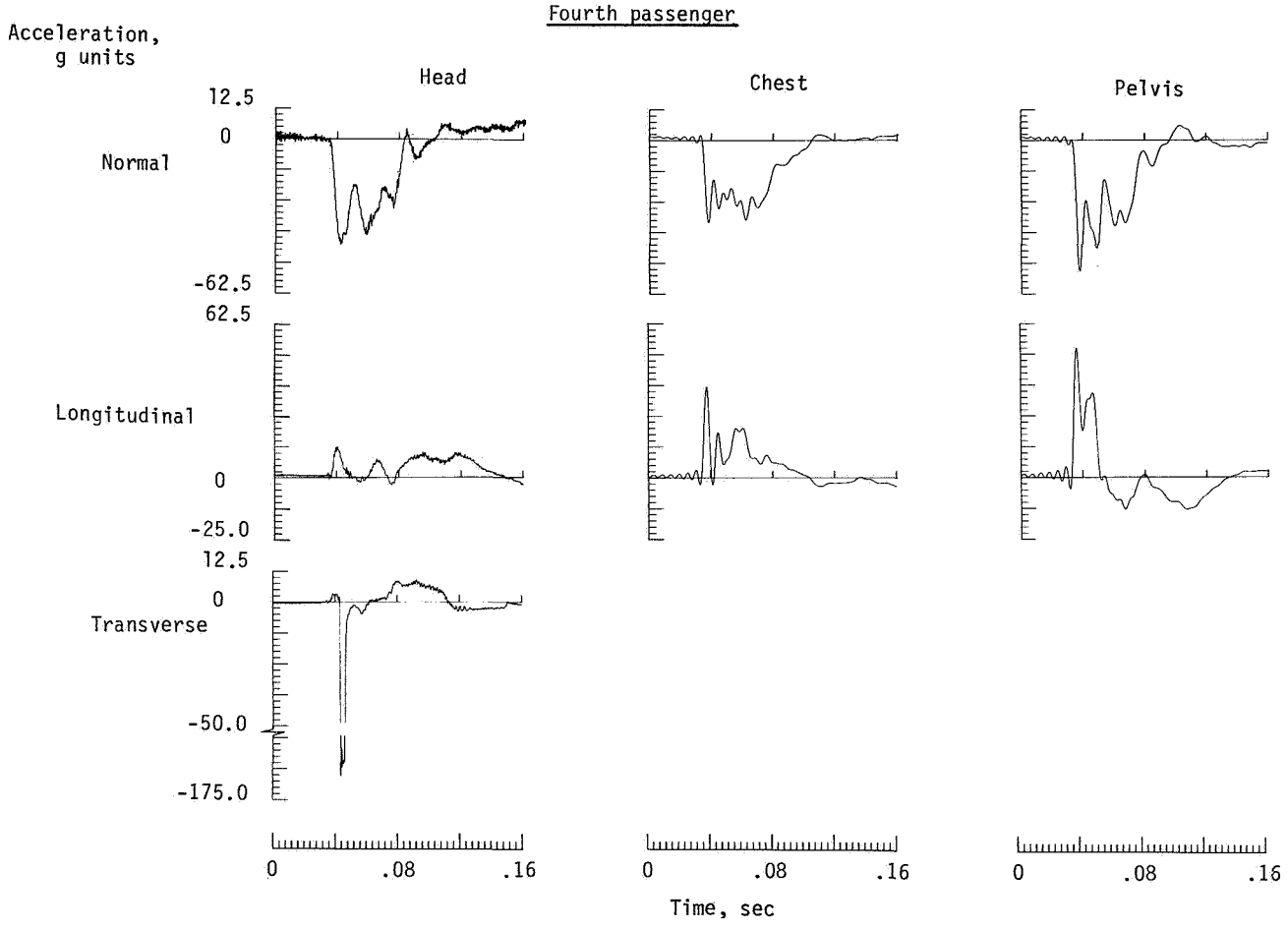

(c) Fourth passenger.

Figure A1. Concluded.

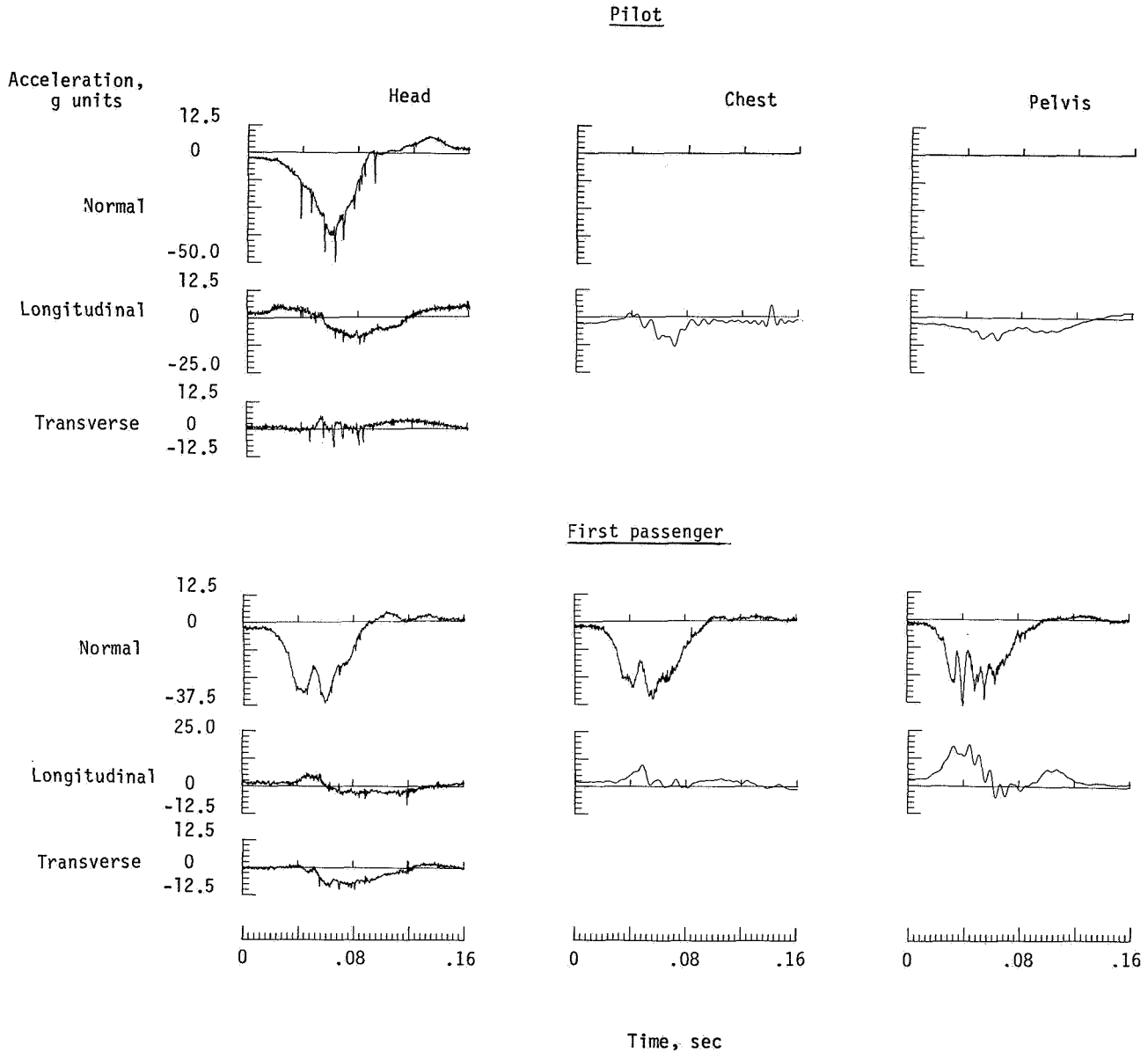

(a) Pilot and first passenger.

Figure A2. Accelerations in anthropomorphic-dummy occupants for the corrugated-beam–notched-corner airplane.

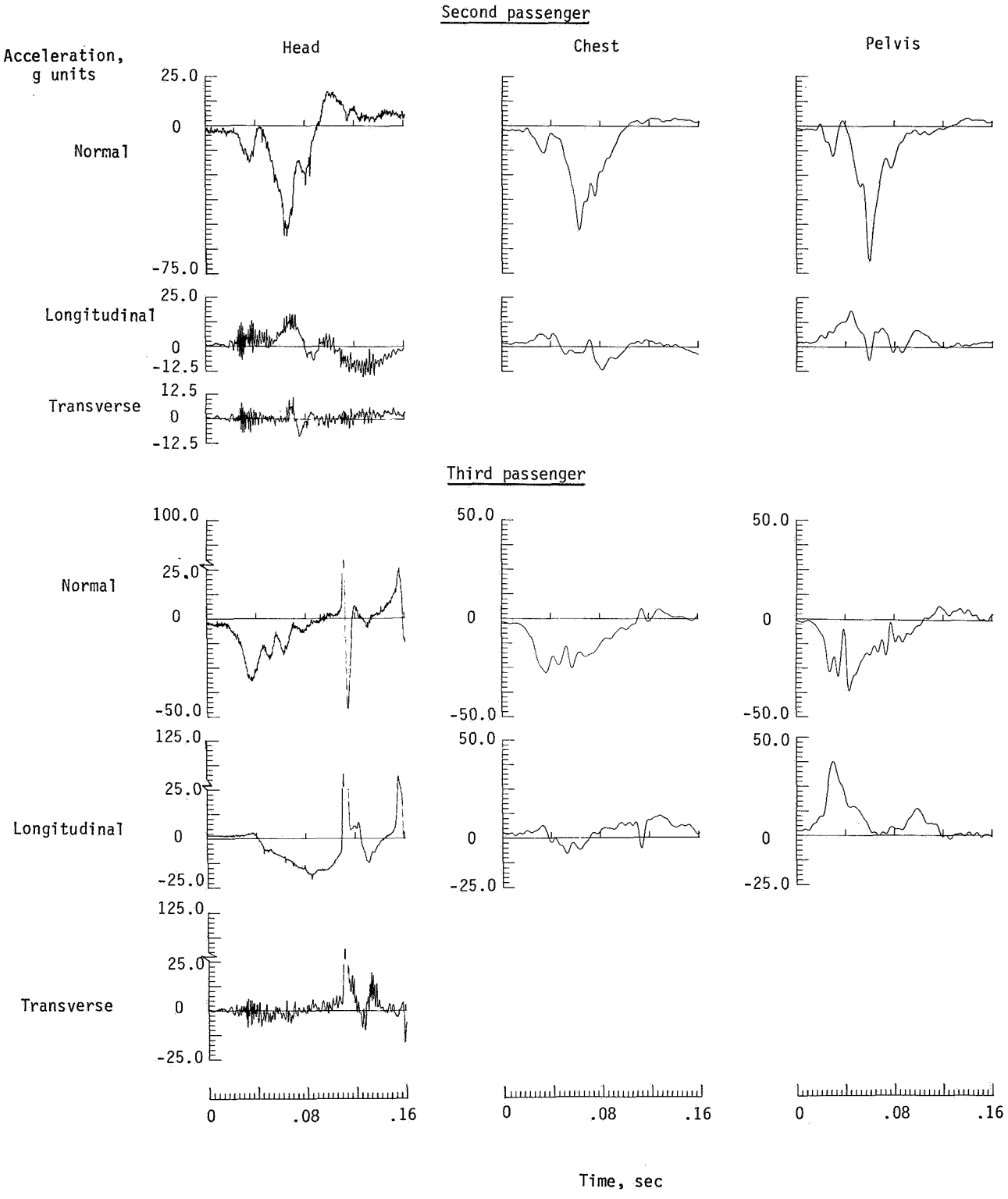

(b) Second and third passengers.

Figure A2. Continued.

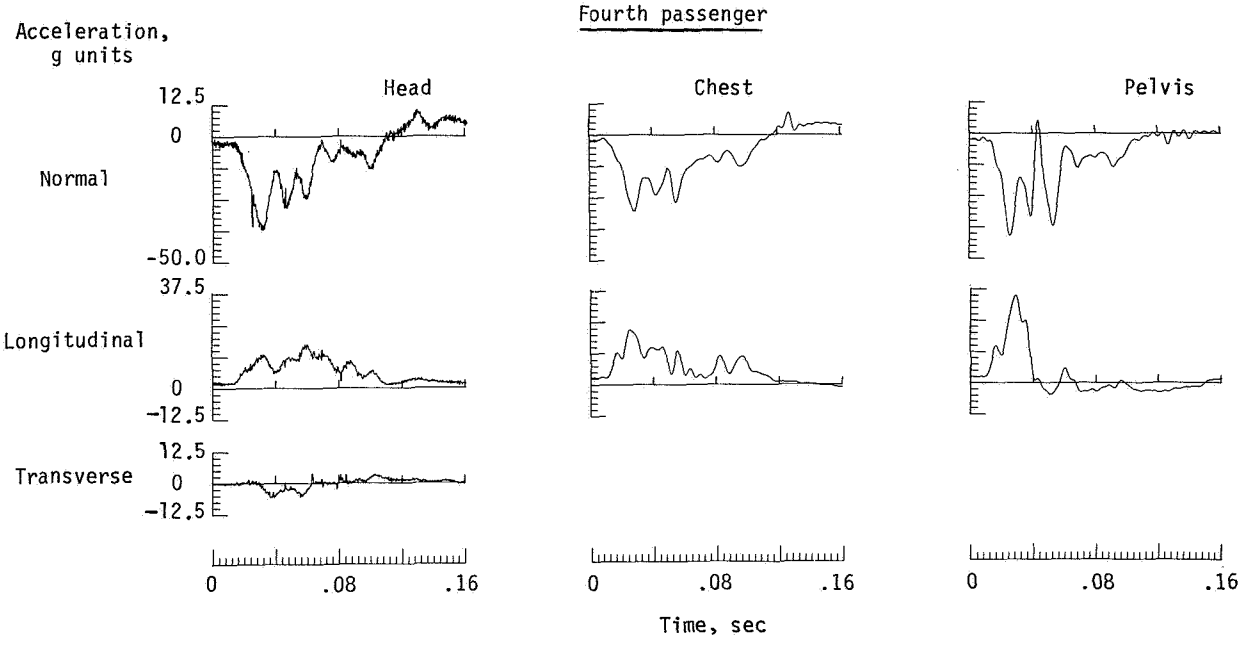

(c) Fourth passenger.

Figure A2. Concluded.

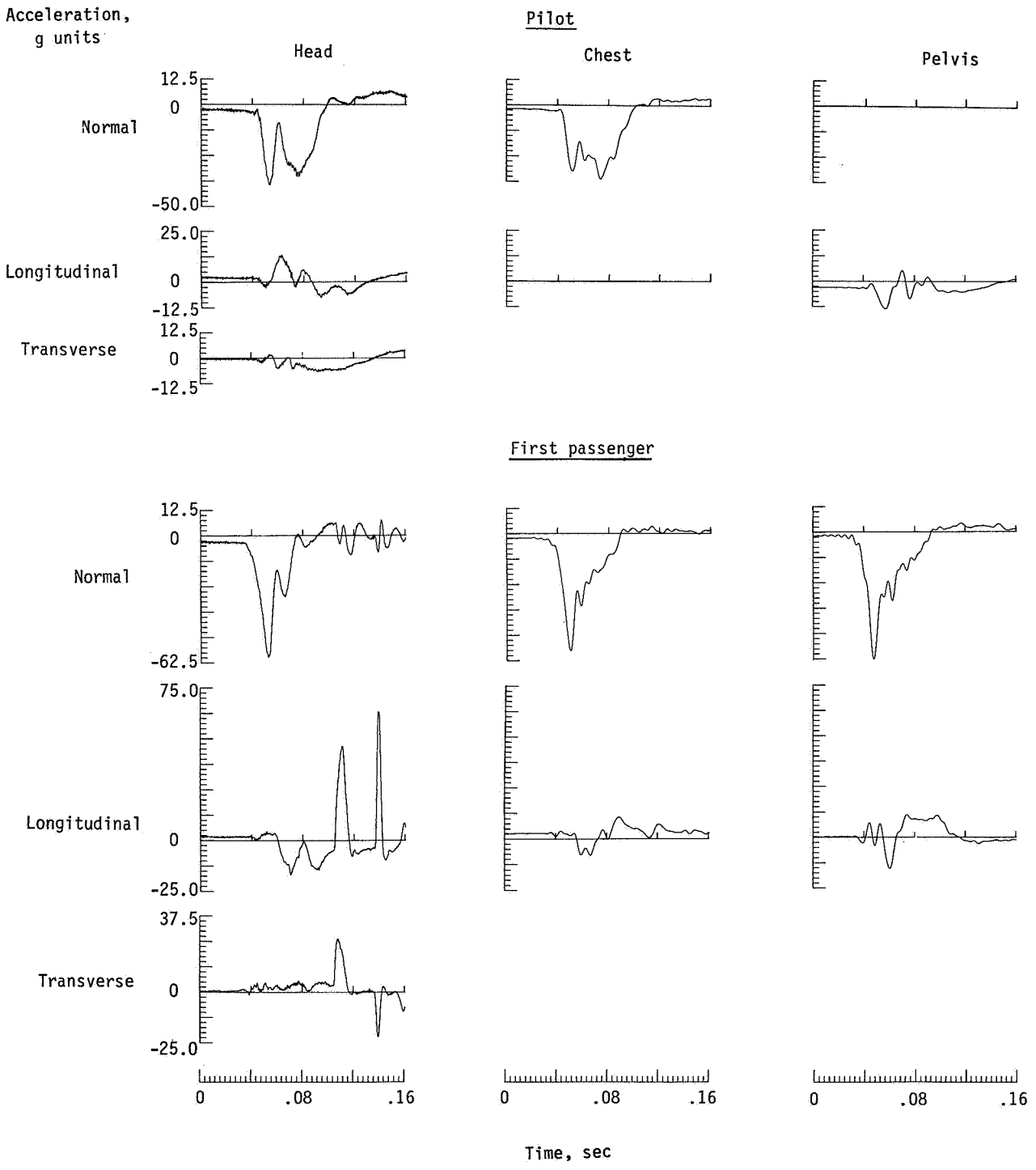

(a) Pilot and first passenger.

Figure A3. Accelerations in anthropomorphic-dummy occupants for notched-corner airplane.

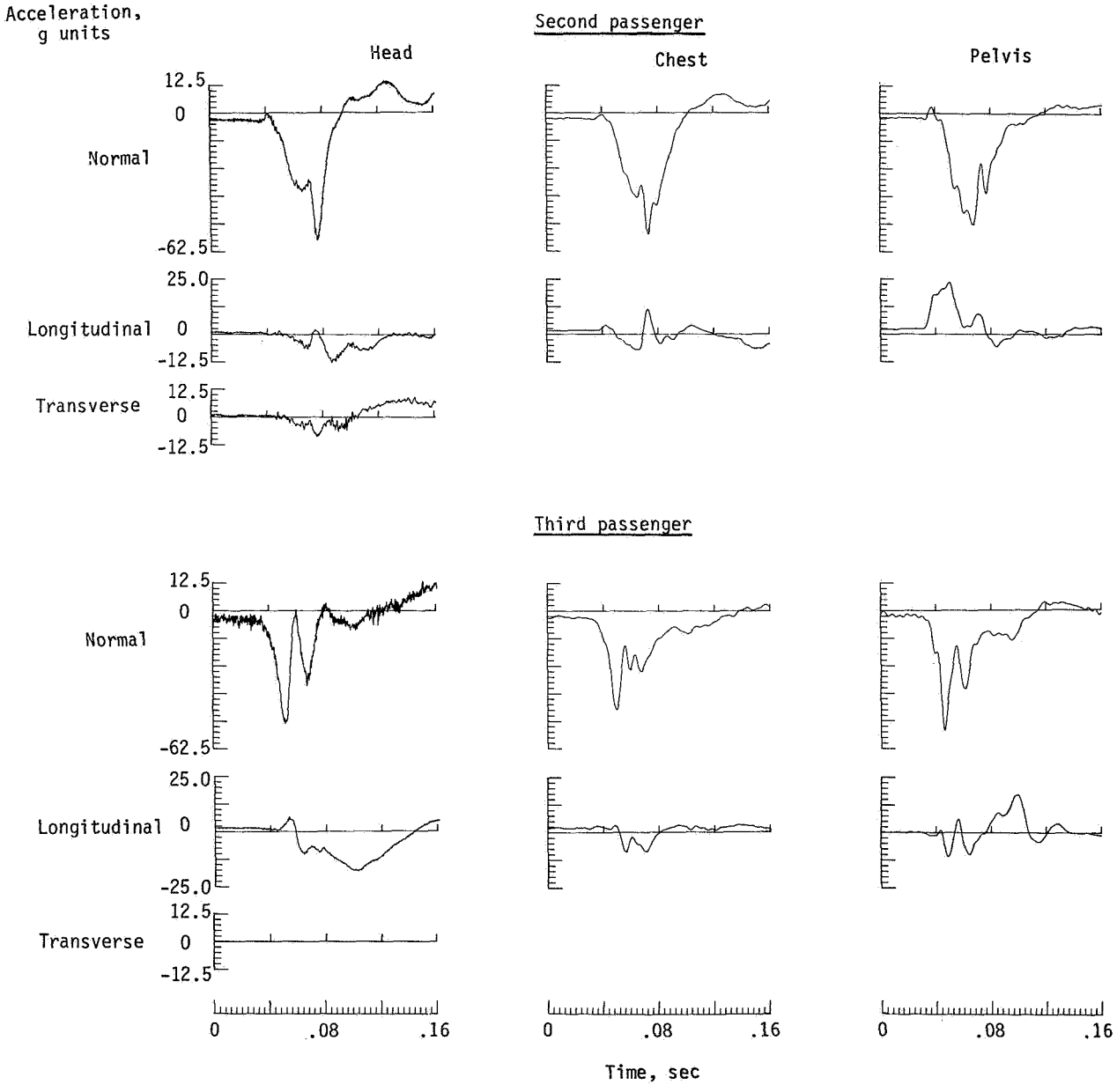

(b) Second and third passengers.

Figure A3. Continued.

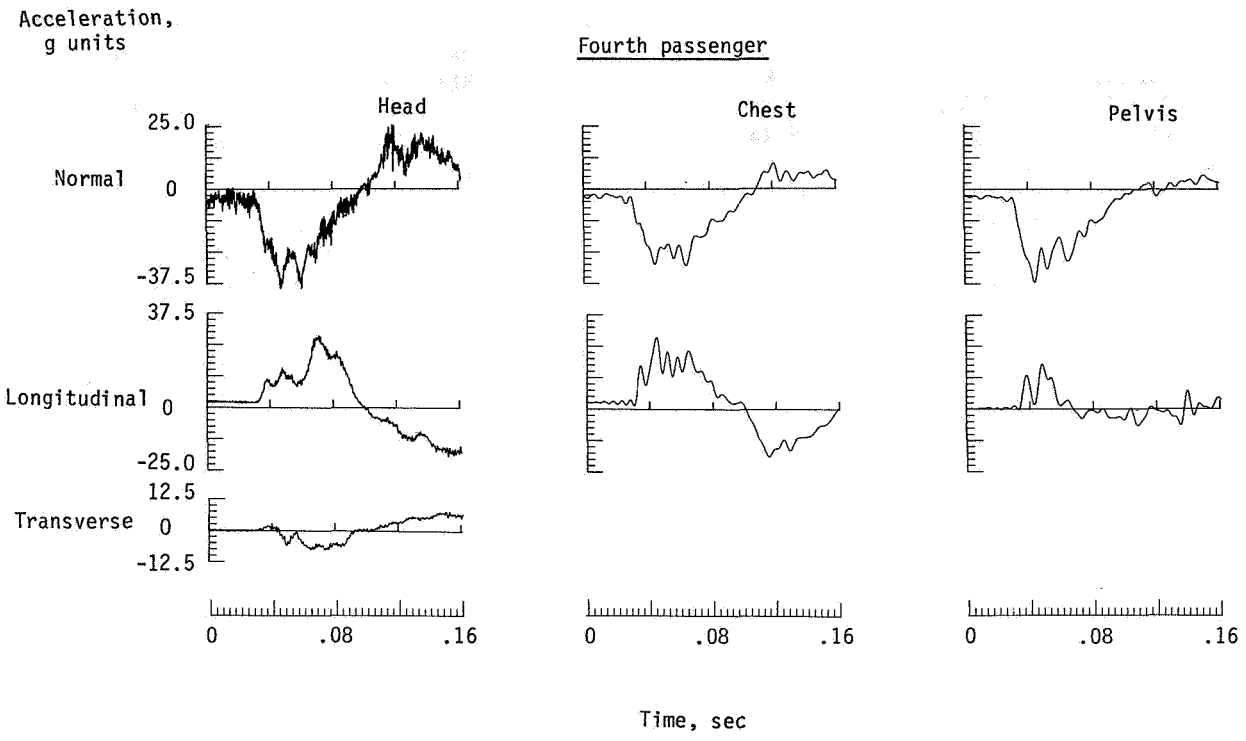

(c) Fourth passenger.

Figure A3. Concluded.

References

1. Alfaro-Bou, Emilio; and Vaughan, Victor L., Jr.: *Light Airplane Crash Tests at Impact Velocities of 13 and 27 m/sec.* NASA TP-1042, 1977.
2. Castle Claude B.; and Alfaro-Bou, Emilio: *Light Airplane Crash Tests at Three Flight-Path Angles.* NASA TP-1210, 1978.
3. Castle, Claude B.; and Alfaro-Bou, Emilio: *Light Airplane Crash Tests at Three Roll Angles.* NASA TP-1477, 1979.
4. Vaughan, Victor L., Jr.; and Alfaro-Bou, Emilio: *Light Airplane Crash Tests at Three Pitch Angles.* NASA TP-1481, 1979.
5. Hayduk, Robert J.; Thomson, Robert G.; and Carden, Huey D.: NASA/FAA General Aviation Crash Dynamics Program—An Update. *Forum,* vol. 12, no. 3, Winter 1979, pp. 147–156.
6. Hayduk, Robert J.: *Comparative Analysis of PA-31-350 Chieftain (N44LV) Accident and NASA Crash Test Data.* NASA TM-80102, 1979.
7. Vaughan, Victor L., Jr.; and Hayduk, Robert J.: *Crash Tests of Four Identical High-Wing Single-Engine Airplanes.* NASA TP-1699, 1980.
8. Carden, Huey D.; and Hayduk, Robert J.: Aircraft Subfloor Response to Crash Loadings. SAE Tech. Paper Ser. 810614, Apr. 1981.
9. Alfaro-Bou, Emilio; Williams, M. Susan; and Fasanella, Edwin L.: Determination of Crash Test Pulses and Their Application to Aircraft Seat Analysis. SAE Tech. Paper 810611, Apr. 1981.
10. Williams, M. Susan; and Fasanella, Edwin L.: *Crash Tests of Four Low-Wing Twin-Engine Airplanes With Truss-Reinforced Fuselage Structure.* NASA TP-2070, 1982.
11. Carden, Huey D.: *Correlation and Assessment of Structural Airplane Crash Data With Flight Parameters at Impact.* NASA TP-2083, 1982.
12. Carden, Huey D.: Impulse Analysis of Airplane Crash Data With Consideration Given to Human Tolerance. SAE Tech. Paper Ser. 830748, Apr. 1983.
13. Cronkhite, James D.: Crashworthy Design Concepts for Airframe Structures of Light Aircraft. SAE Paper 810613, Apr. 1981.
14. Cronkhite, J. D.; and Berry, V. L.: *Crashworthy Airframe Design Concepts—Fabrication and Testing.* NASA CR-3603, 1982.
15. Vaughan, Victor L., Jr.; and Alfaro-Bou, Emilio: *Impact Dynamics Research Facility for Full-Scale Aircraft Crash Testing.* NASA TN D-8179, 1976.
16. Anthropomorphic Test Dummies. Transportation, Code of Federal Regulations, Title 49, Chapter VI, Part 572, U.S. Govt. Printing Off., Oct. 1, 1981, pp. 421–443.
17. Eiband, A. Martin: *Human Tolerance to Rapidly Applied Accelerations: A Summary of the Literature.* NASA MEMO 5-19-59E, 1959.

TABLE I. VERTICAL STROKES FOR LOAD-LIMITING SEATS IN TEST AIRPLANES

Position/seat type	Seat vertical stroke, cm (in.), for—		
	Unmodified subfloor	Notched-corner subfloor	Corrugated-beam–notched-corner subfloor
Pilot/S-leg	Front leg—14.2 (5.6) Rear leg—6.6 (2.6)	Front leg—10.7 (4.2) Rear leg—7.1 (2.8)	Front leg—9.9 (3.9)
Second passenger/ composite tube	> 15.2 (> 6.0)*	≈ 15.2 (≈ 6.0)	≈ 15.2 (≈ 6.0)
Fourth passenger/ wire bending	Inboard leg—16.5 (6.5) Outboard leg—12.4 (4.9)	Inboard leg—9.9 (3.9) Outboard leg—7.2 (2.85)	Inboard leg—8.3 (3.25) Outboard leg—6.4 (2.5)

*Bottomed out.

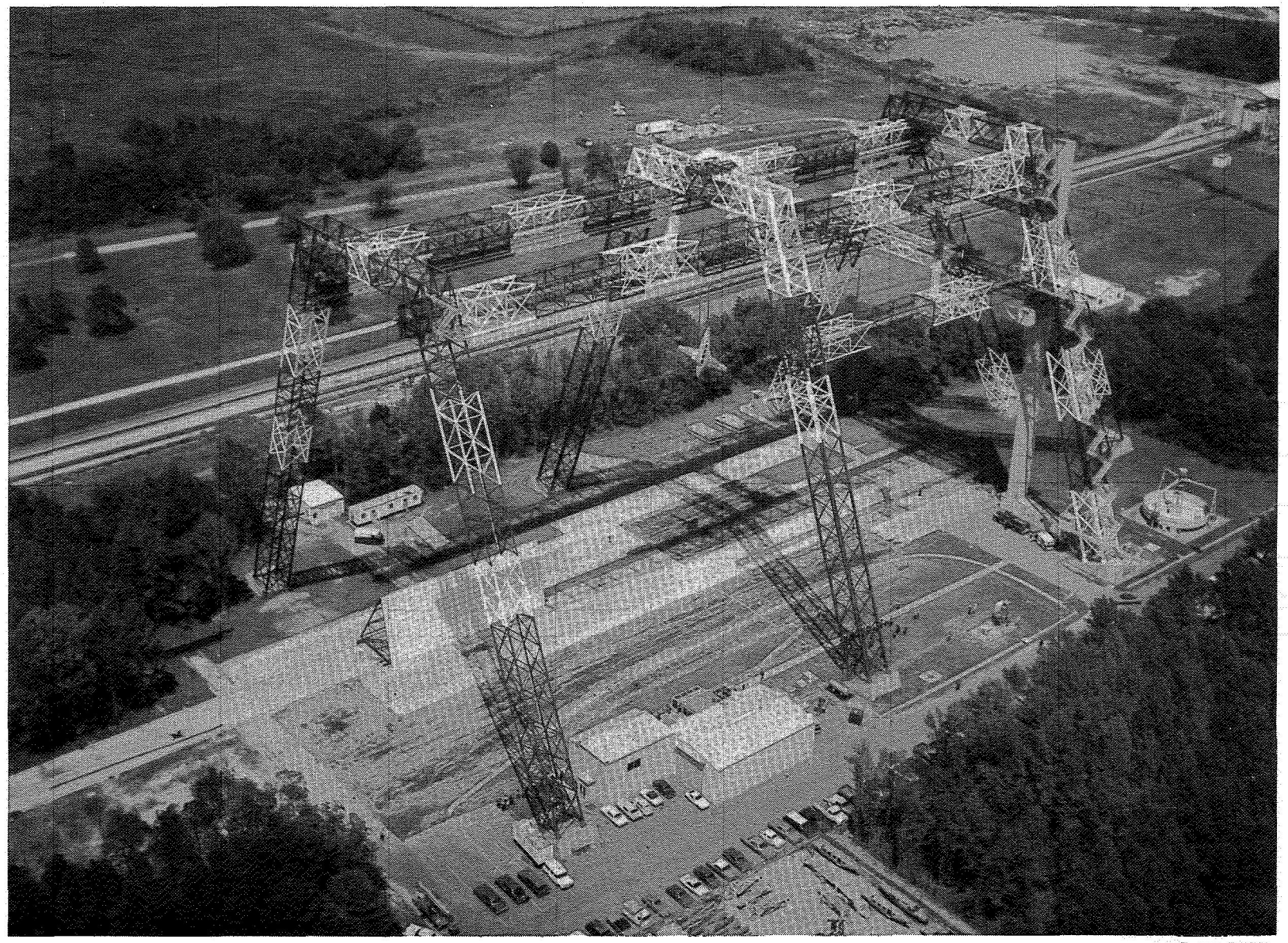

L-74-2505

Figure 1. Langley Impact Dynamics Research Facility.

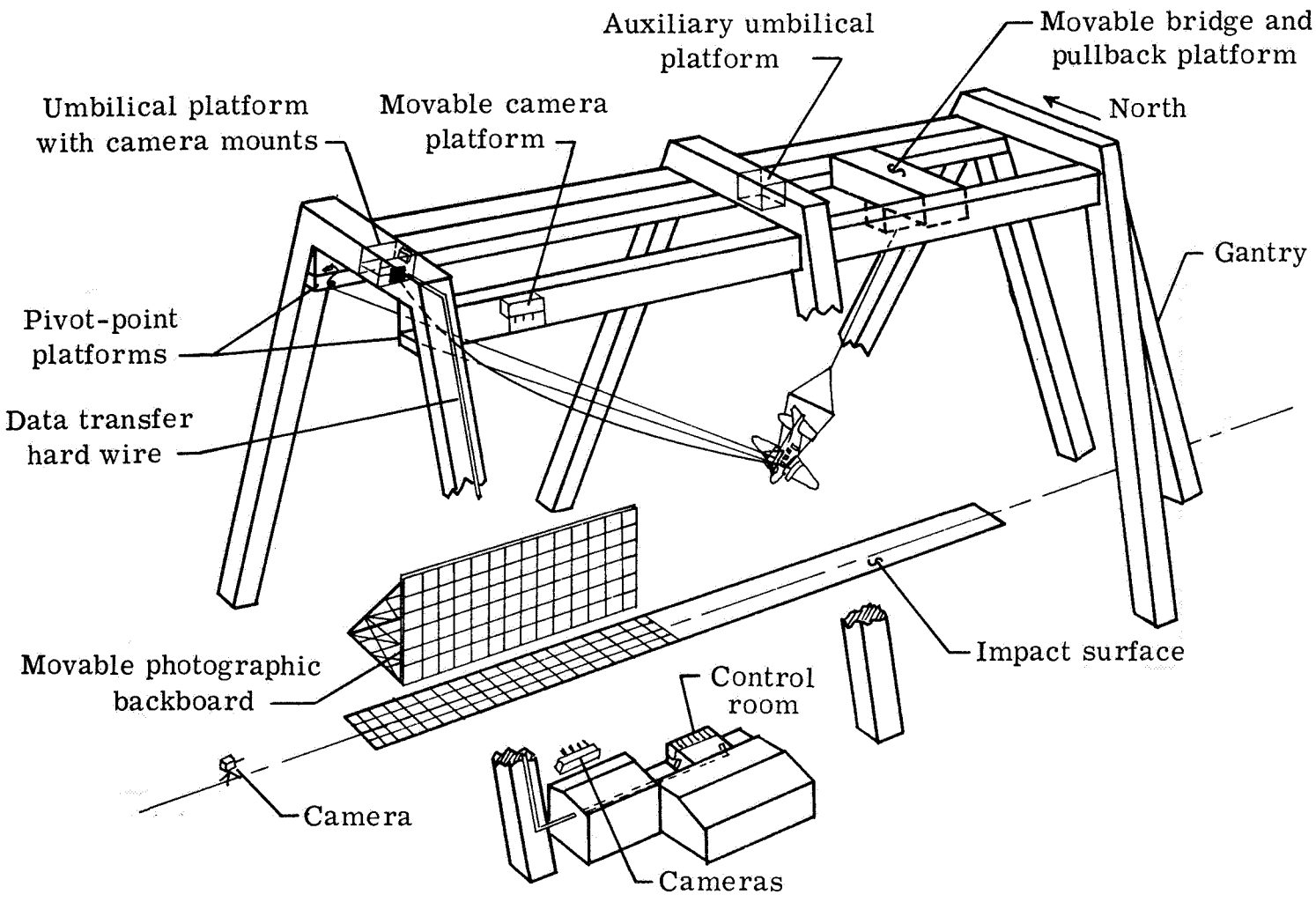

Figure 2. Diagram of Langley Impact Dynamics Research Facility.

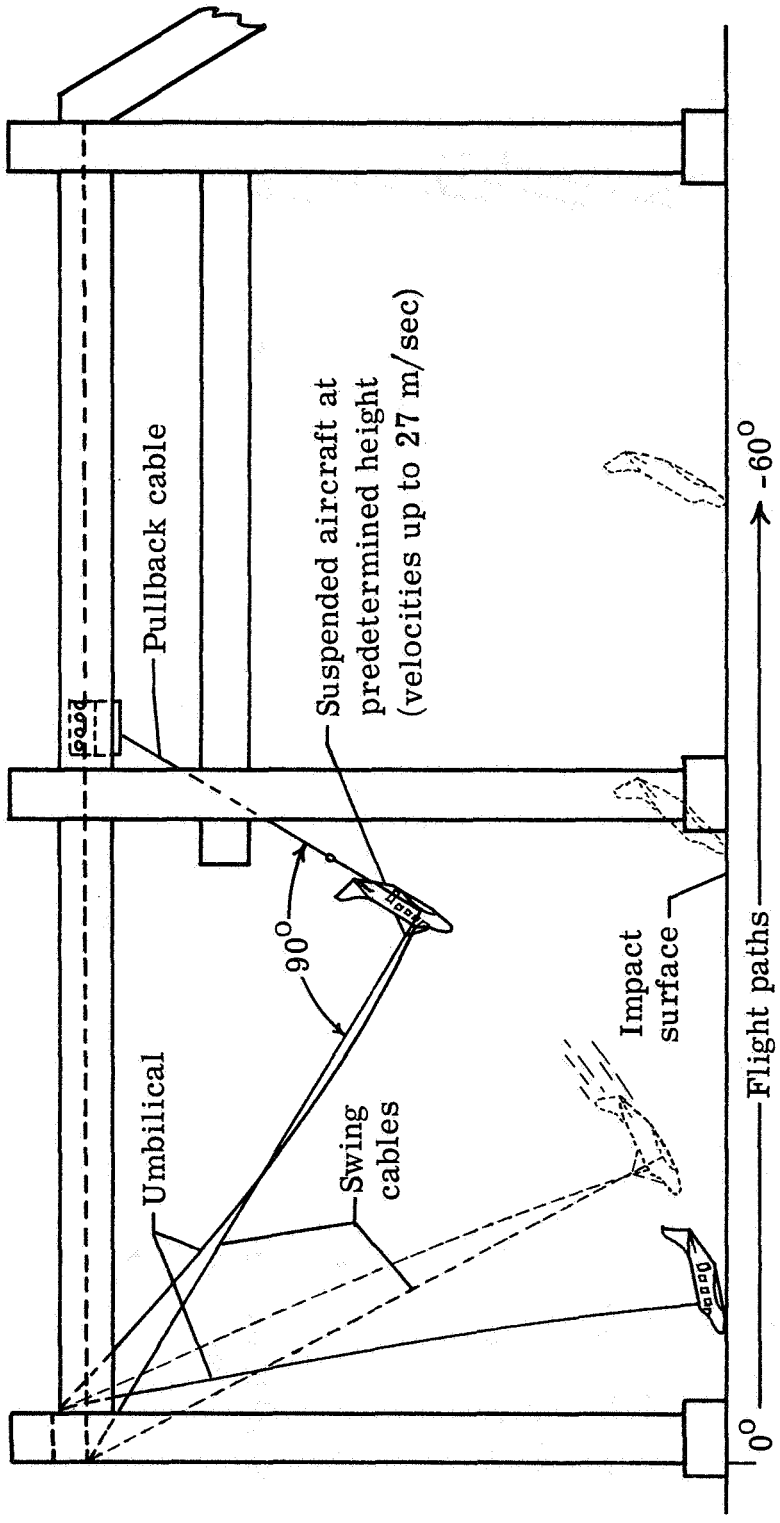

Figure 3. Full-scale airplane crash-test technique.

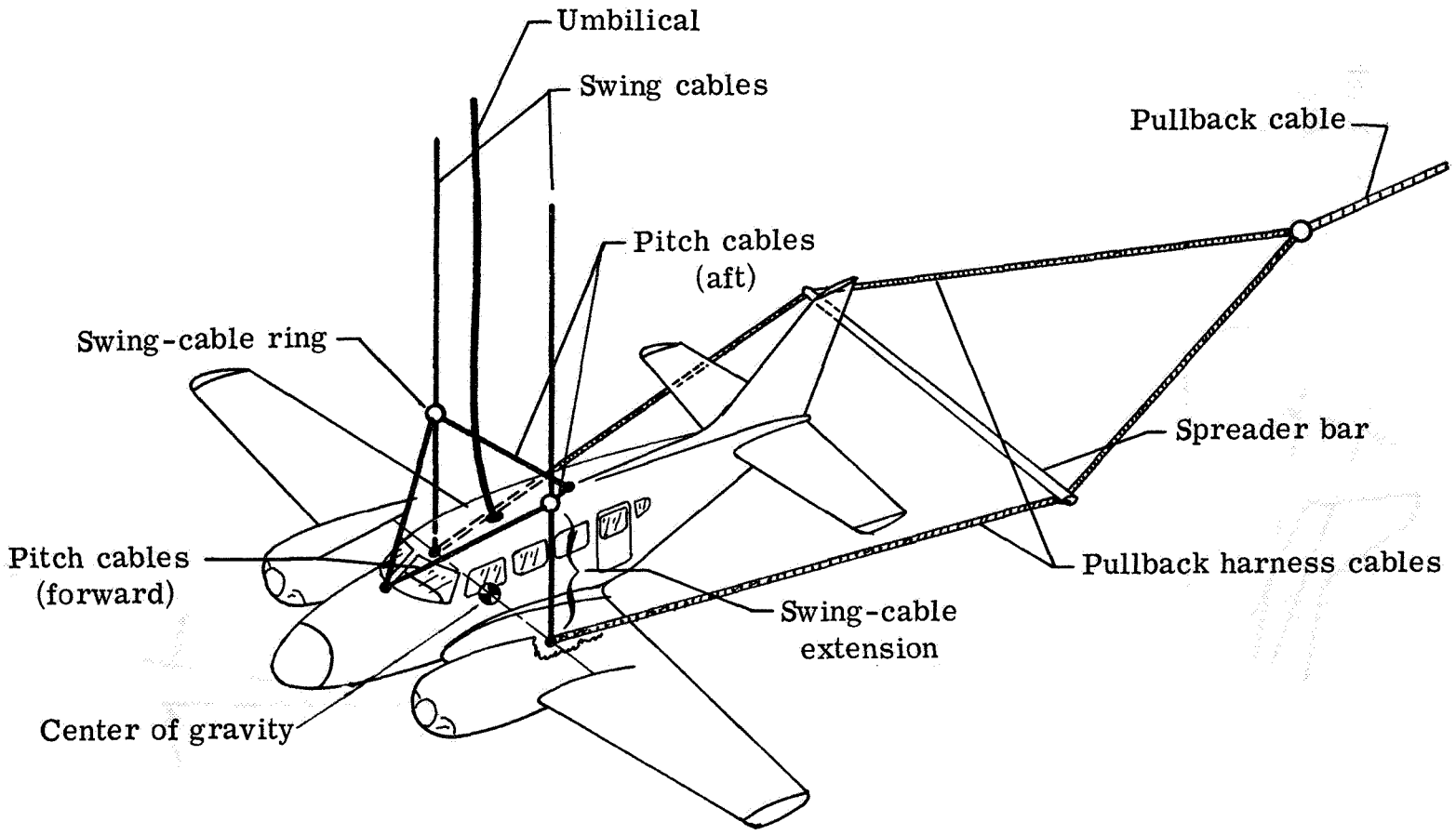

Figure 4. Airplane suspension system.

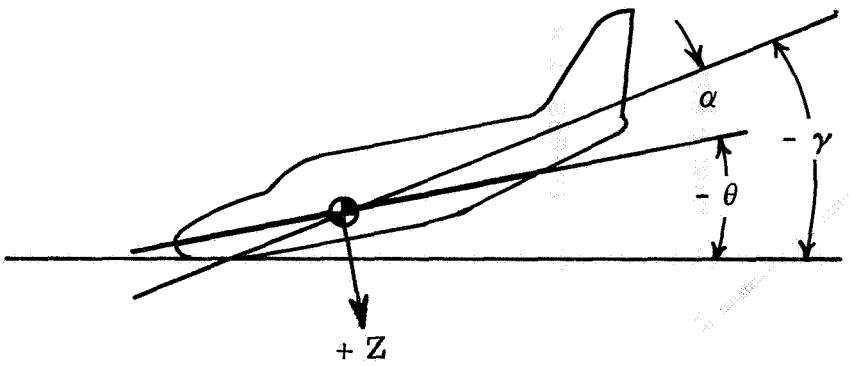

γ Flight-path angle
α Angle of attack
θ Pitch angle,
$\theta = \gamma + \alpha$

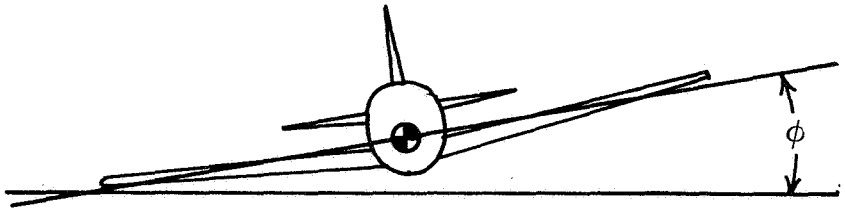

ϕ Roll angle

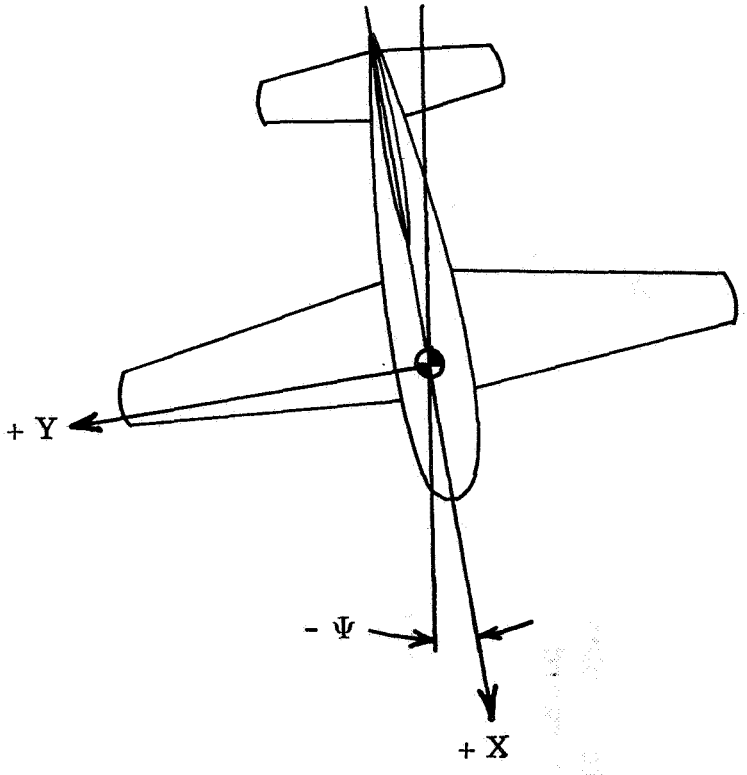

Ψ Yaw angle

Figure 5. Definition of flight path, crash attitudes, axes, and force directions.

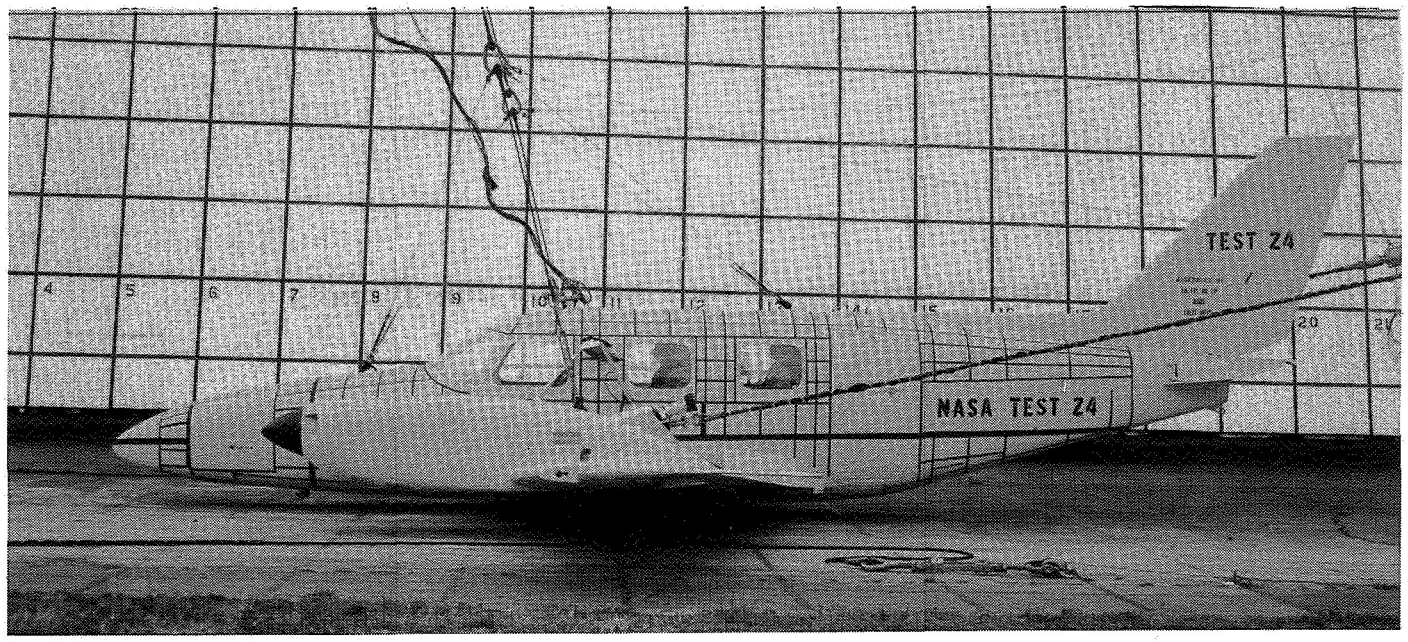

Crash-test attitudes

Test variable	Unmodified floor	Corrugated-beam—notched-corner floor	Notched-corner floor
Flight-path angle, deg	-15.0	-15.0	-15.0
Angle of attack, deg	15.0	16.2	17.5
Pitch angle, deg	0	1.2	2.5
Roll angle, deg	0	6.0	-3.5
Yaw angle, deg	-2.0	6.0	2.2
Flight-path velocity, m/sec	33.7	36.4	37.9
Horizontal velocity, m/sec	32.6	35.2	36.6
Vertical velocity, m/sec	8.7	9.4	9.8

L-84-129

Figure 6. Photograph of airplane in crash-test attitude and tabulation of parameters.

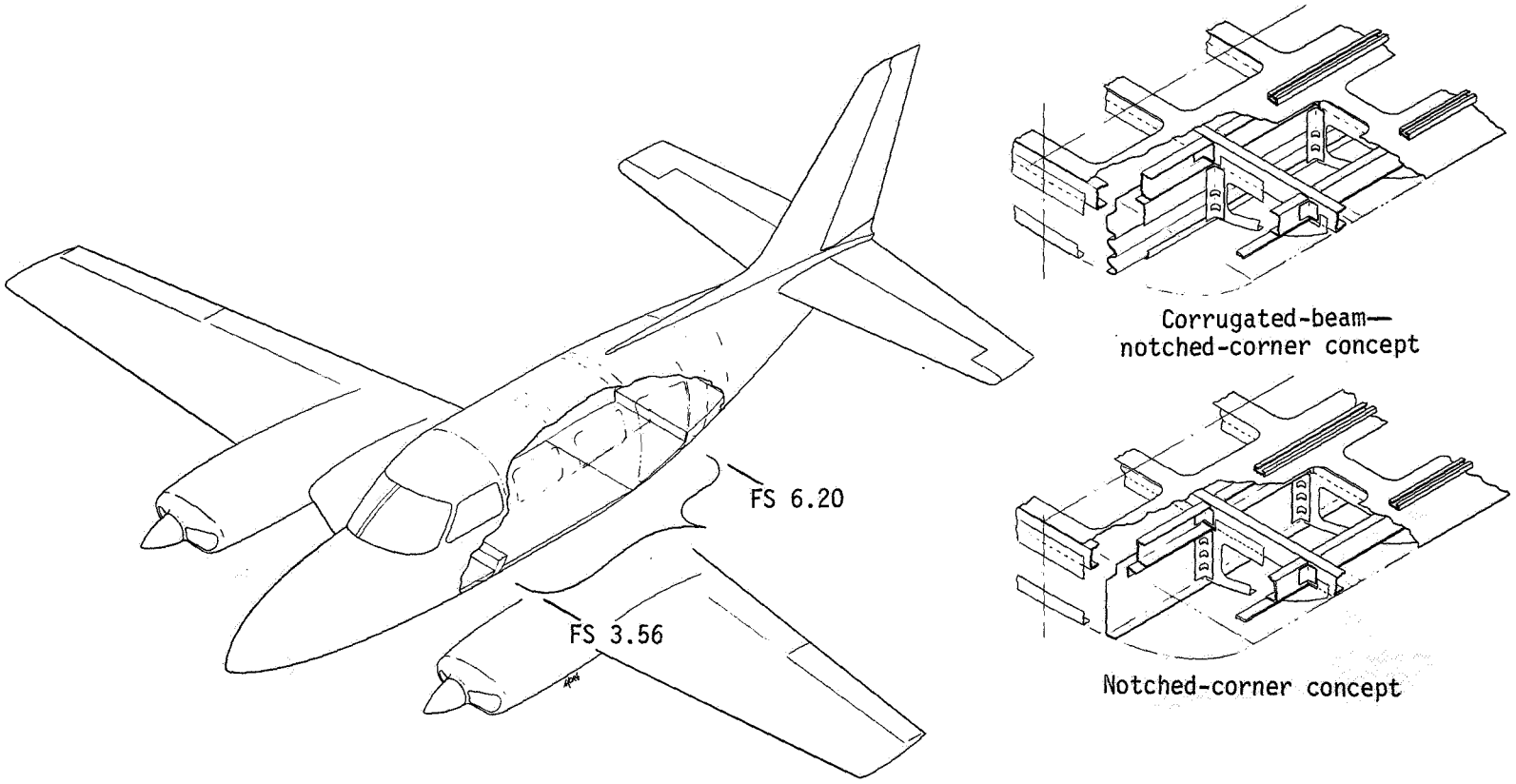

Figure 7. Fuselage modification schematic. Dimensions are in meters.

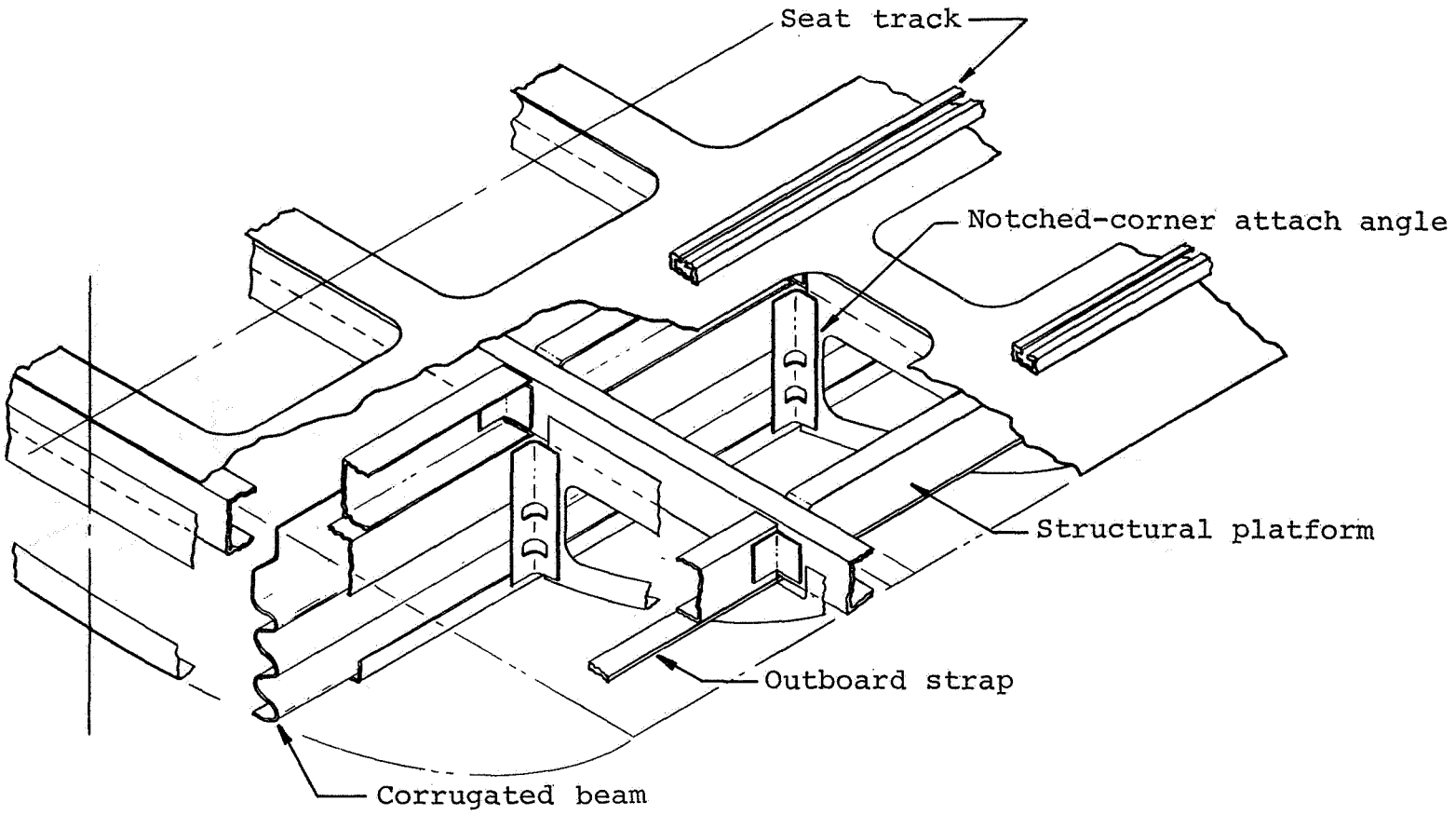

Figure 8. Fuselage modification detail of corrugated-beam–notched-corner structure.

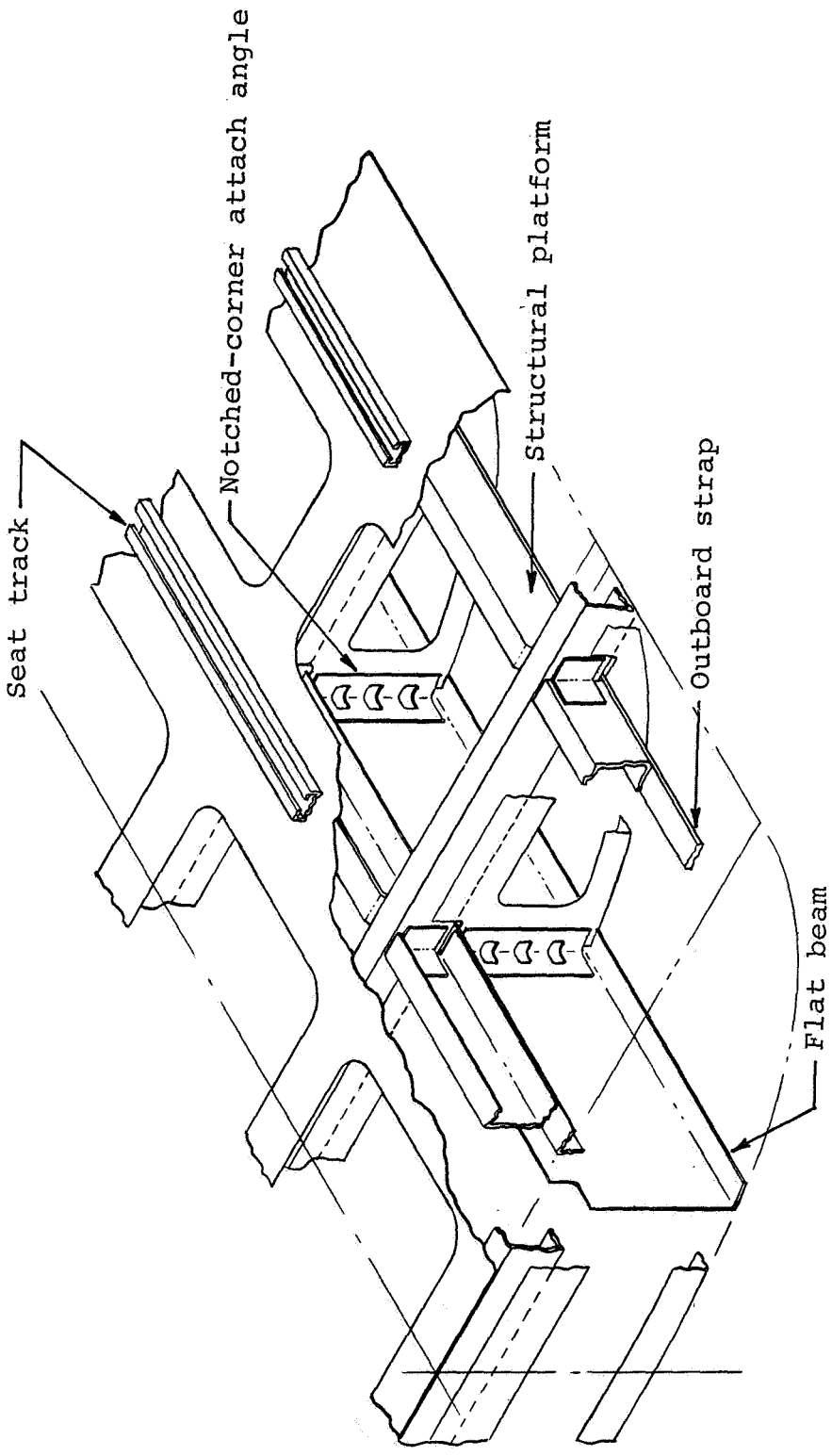

Figure 9. Fuselage modification detail of notched-corner structure.

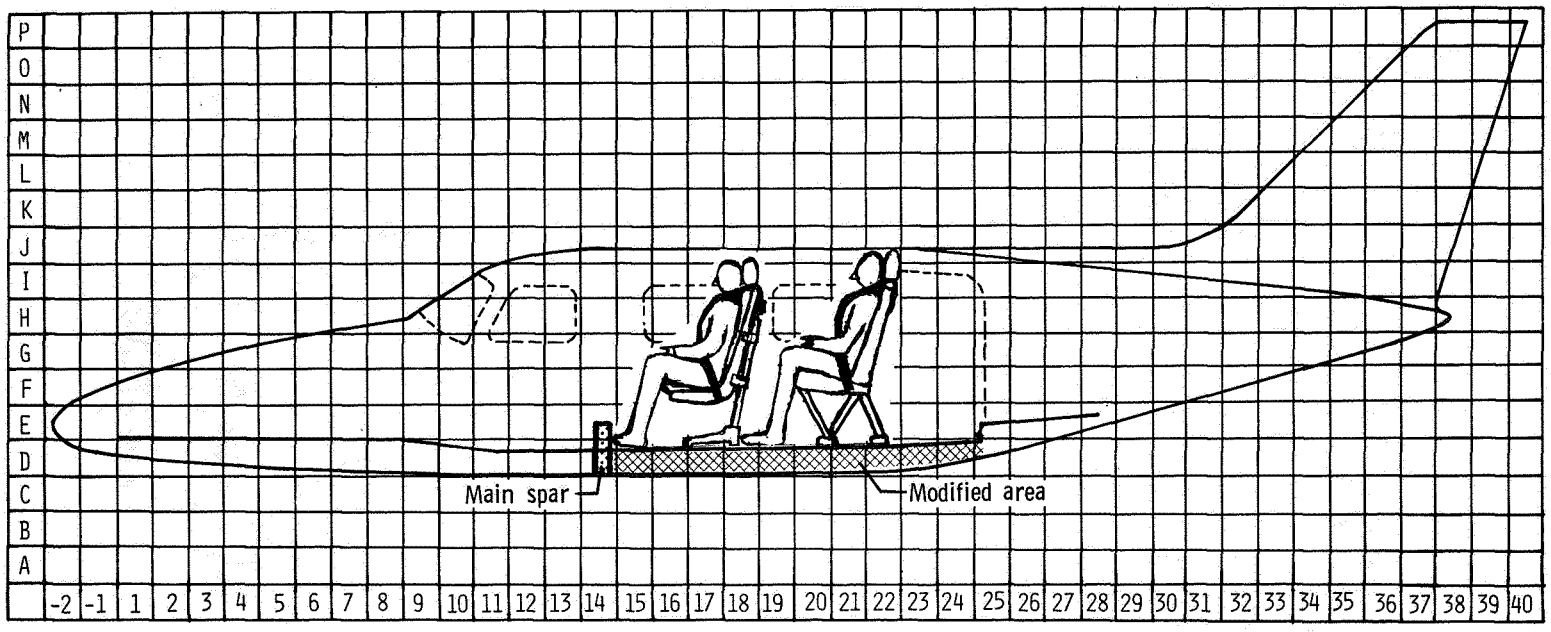

(a) Starboard side—second and fourth passengers.

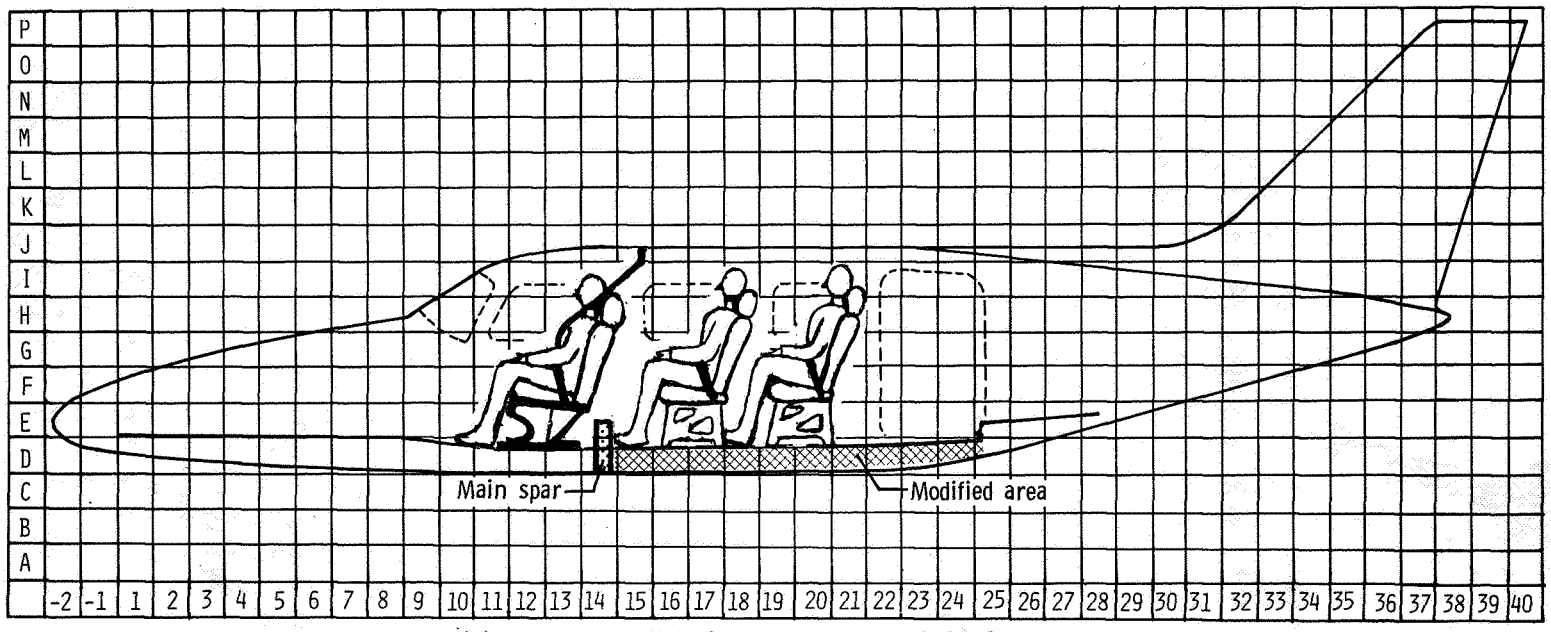

(b) Port side—pilot, first passenger, and third passenger.

Figure 10. Arrangement of anthropomorphic dummies and seats.

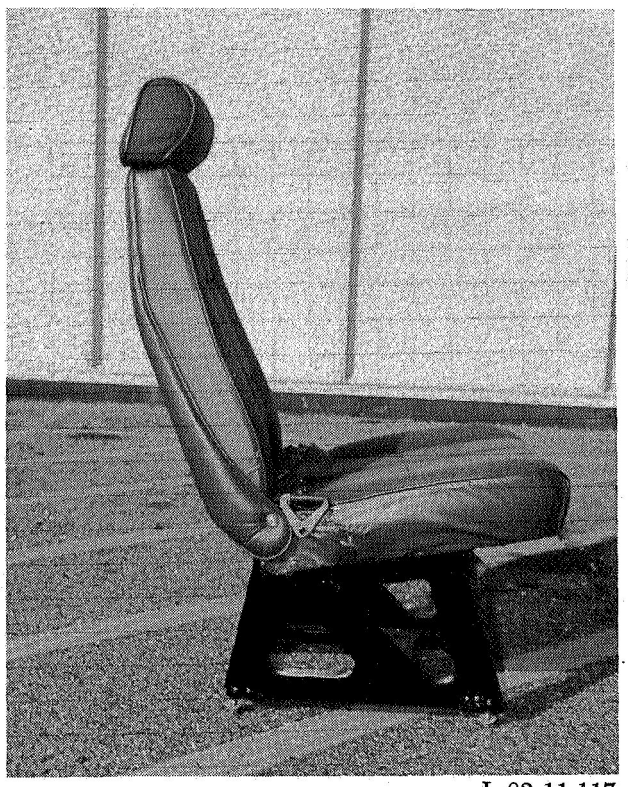

L-82-11,117

(a) Standard seat (first and third passengers).

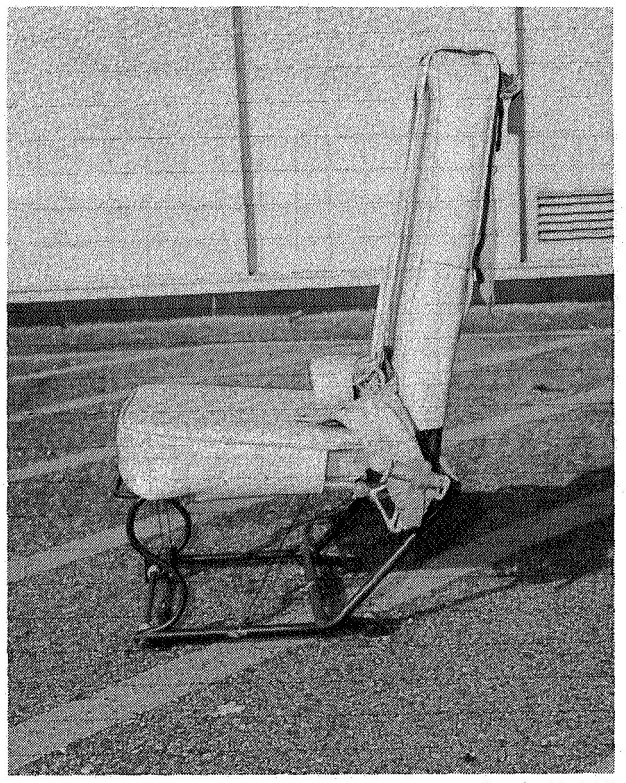

L-82-11,118

(b) Load-limiting seat with S-shaped legs (pilot).

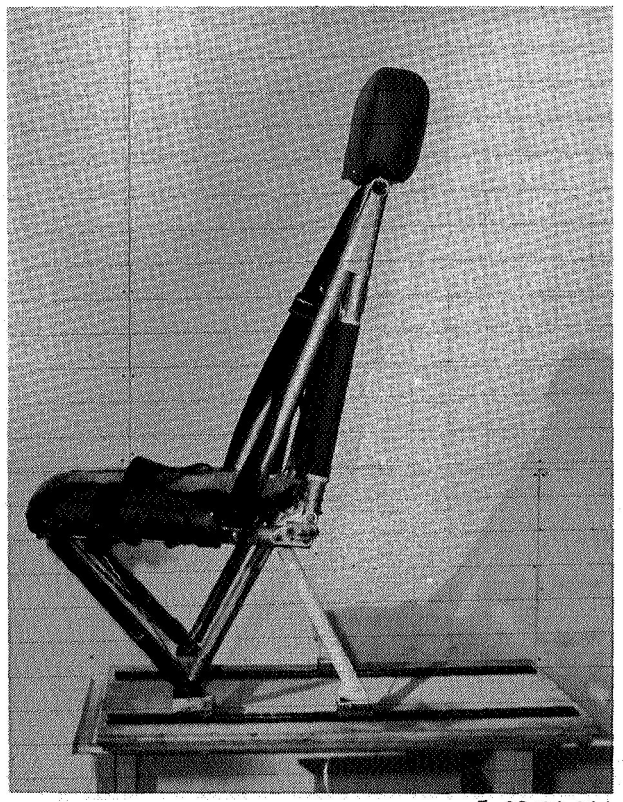

L-82-11,114

(c) Wire-bending load-limiting seat (fourth passenger).

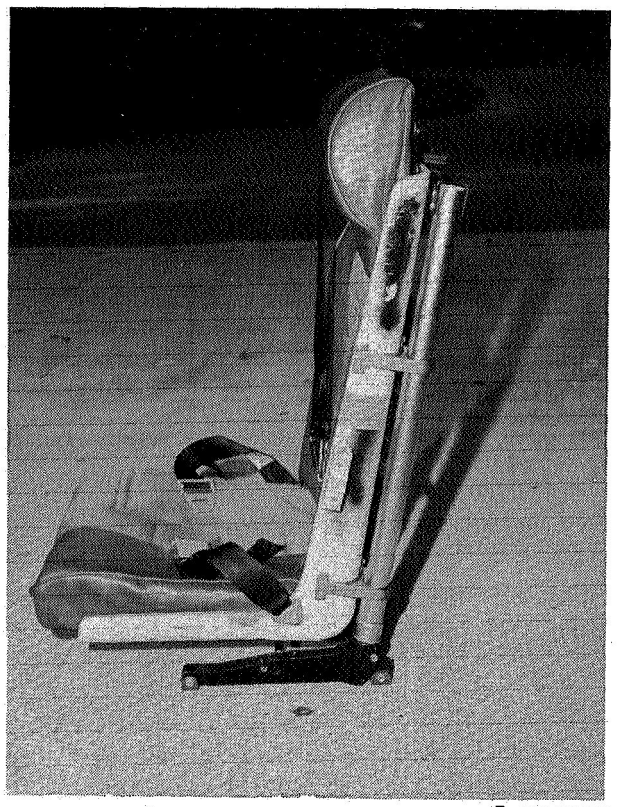

L-82-9980

(d) Composite-tube load-limiting seat (second passenger).

Figure 11. Seat types used in airplane test series.

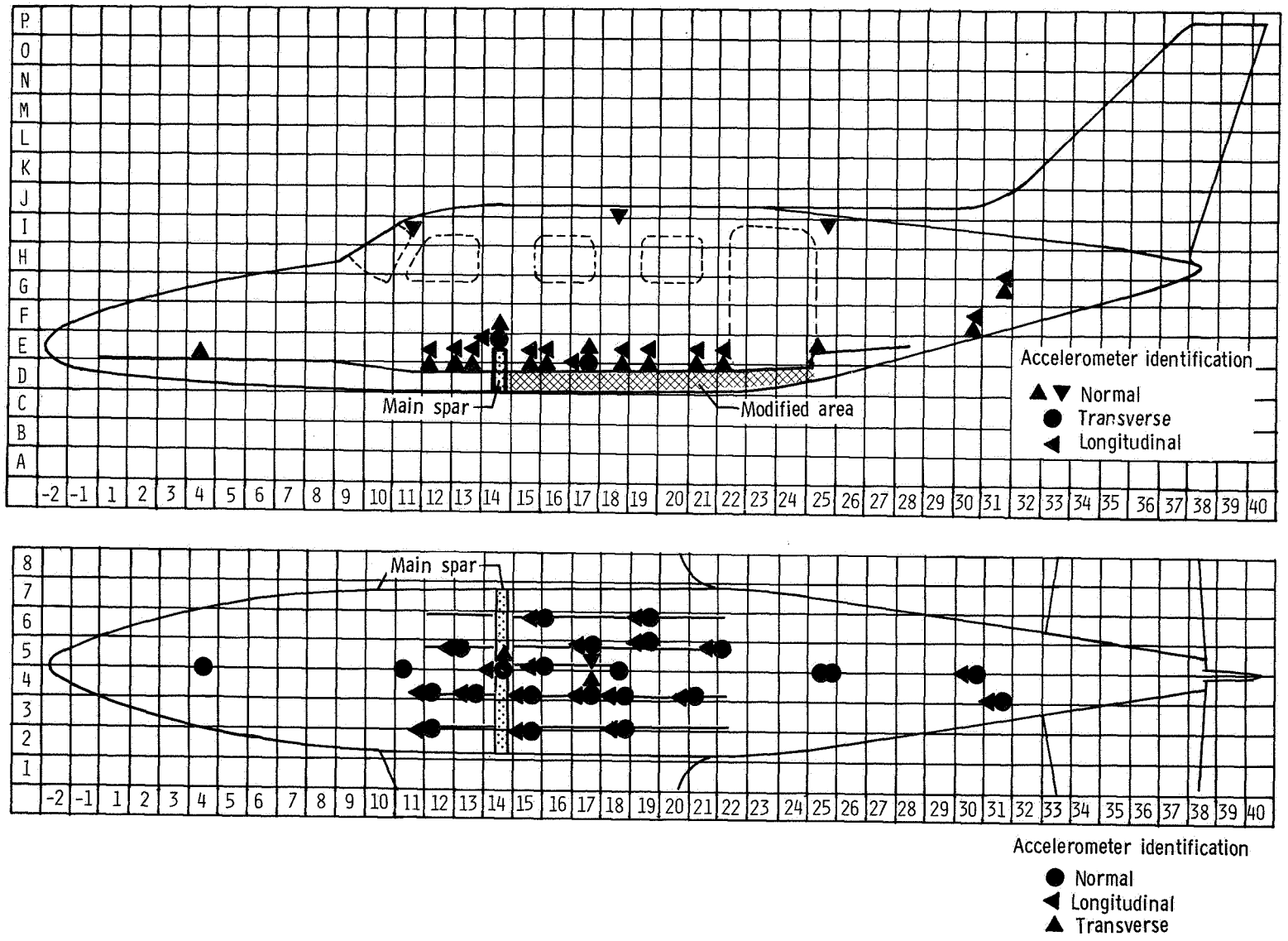

(a) Structural locations.

Figure 12. Accelerometer locations on test airplanes and in anthropomorphic dummies.

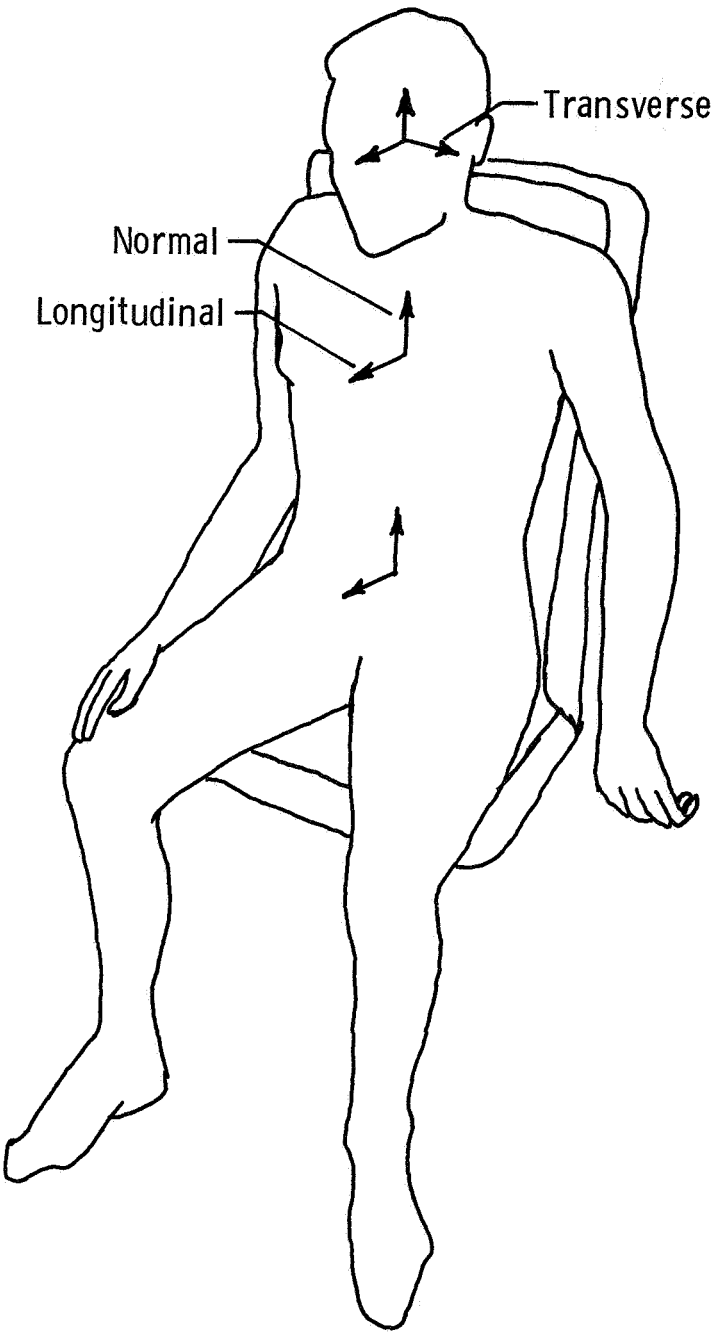

(b) Anthropomorphic dummy.

Figure 12. Concluded.

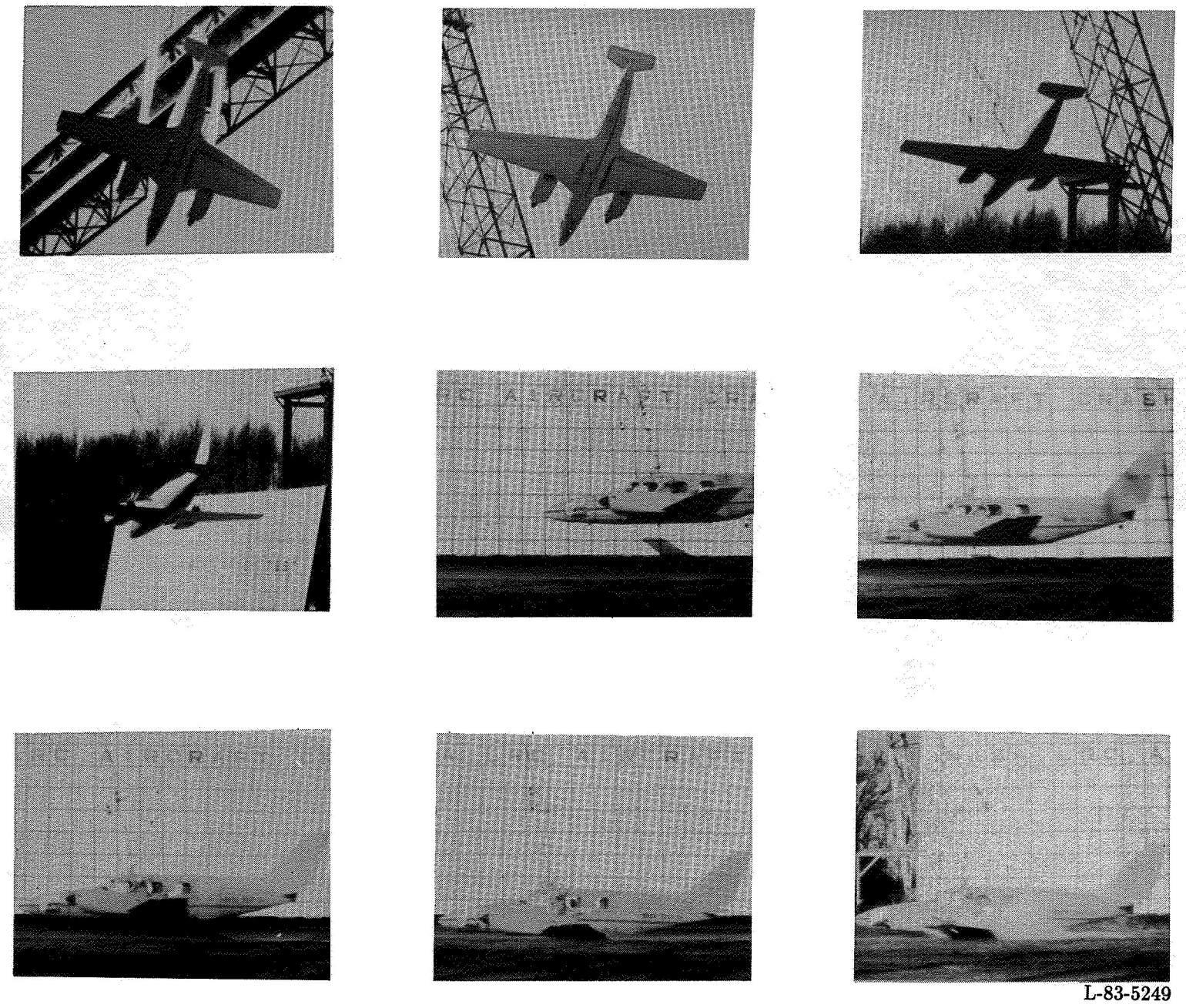

L-83-5249

Figure 13. Typical crash sequence of test airplane (unspecified time intervals).

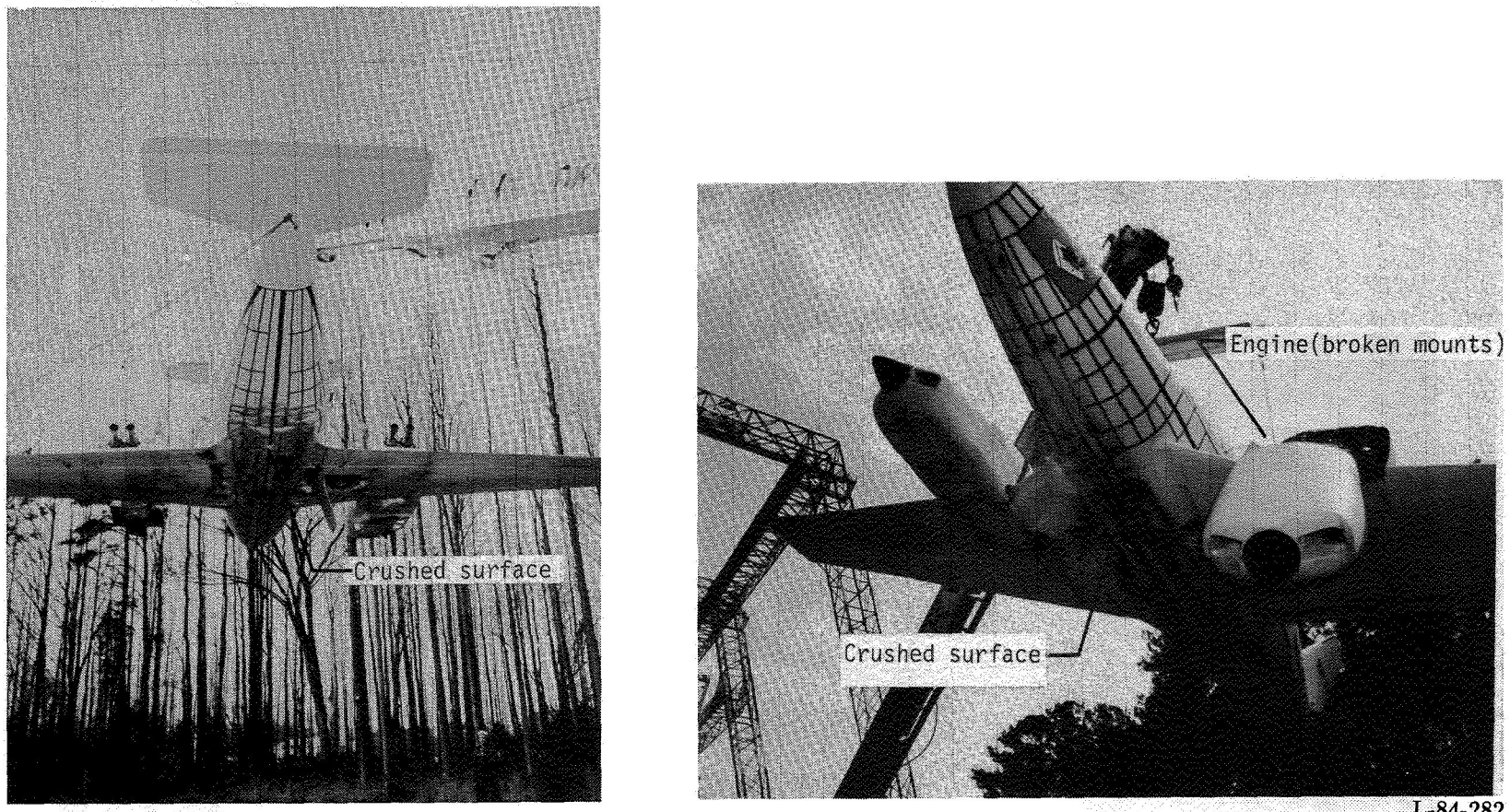

Figure 14. Underside of two test airplanes showing damage.

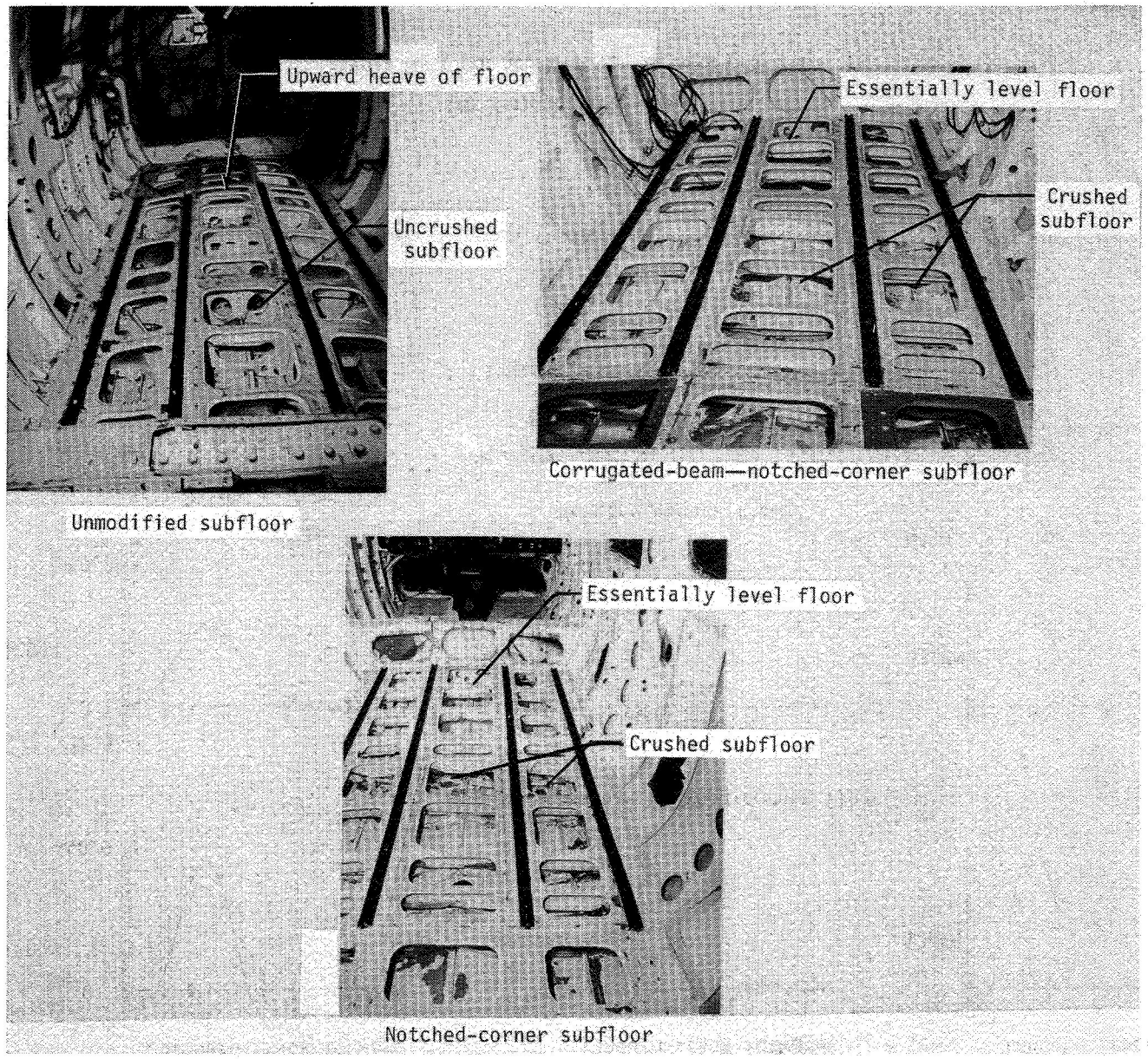

L-84-283

Figure 15. Photographs of interior of airplanes showing floor structure.

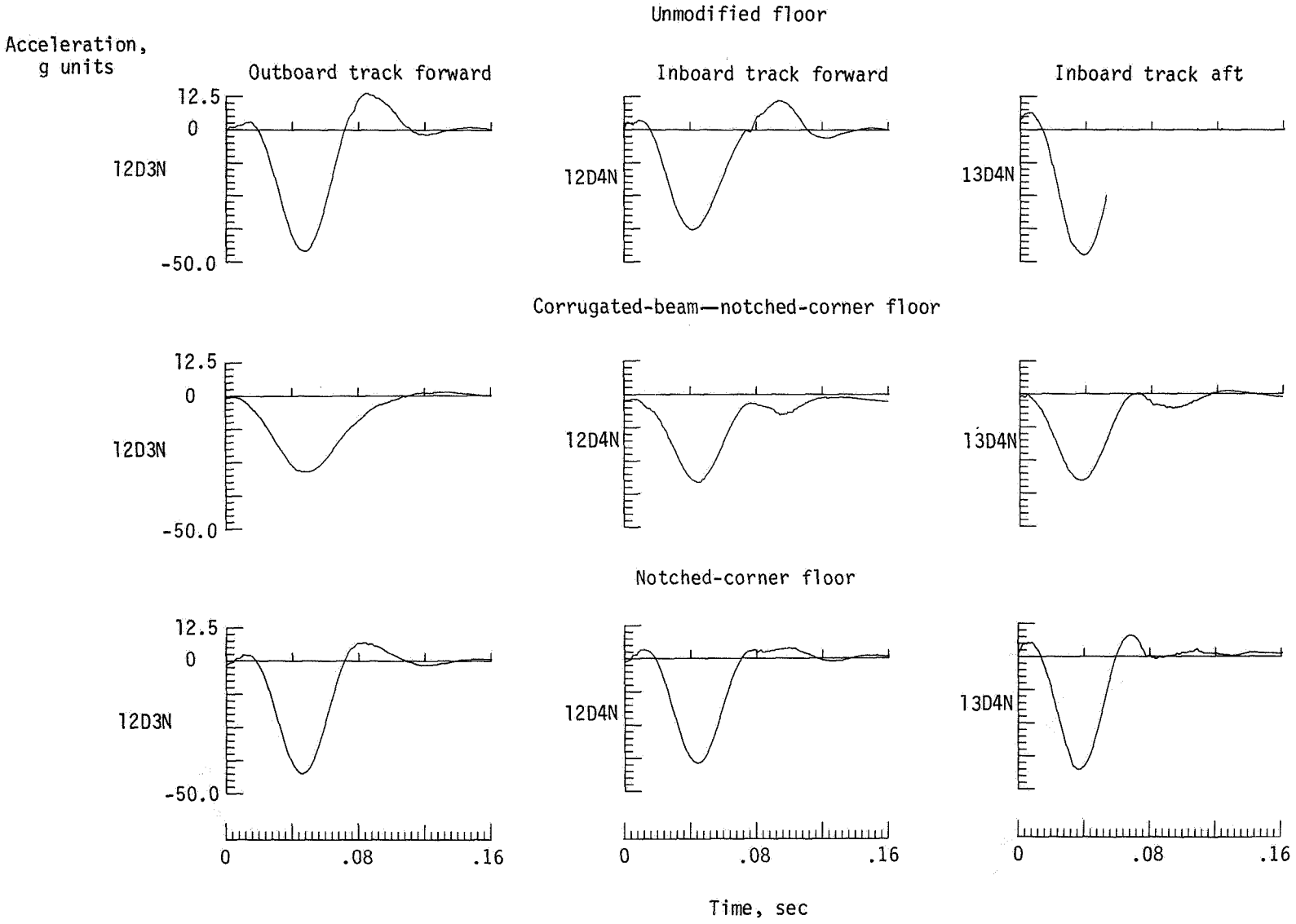

(a) Normal accelerations.

Figure 16. Floor accelerations for pilot position.

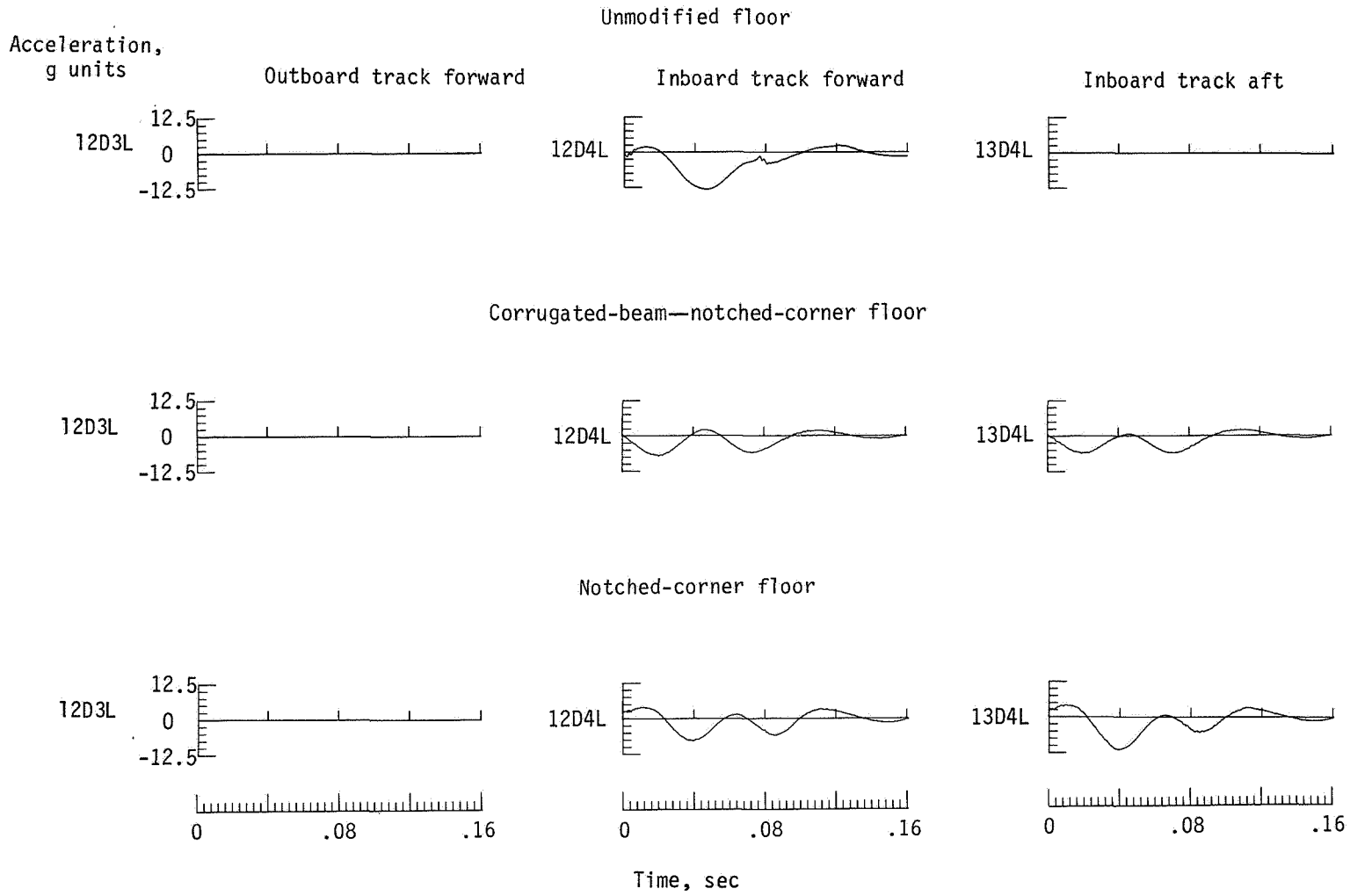

(b) Longitudinal accelerations.

Figure 16. Concluded.

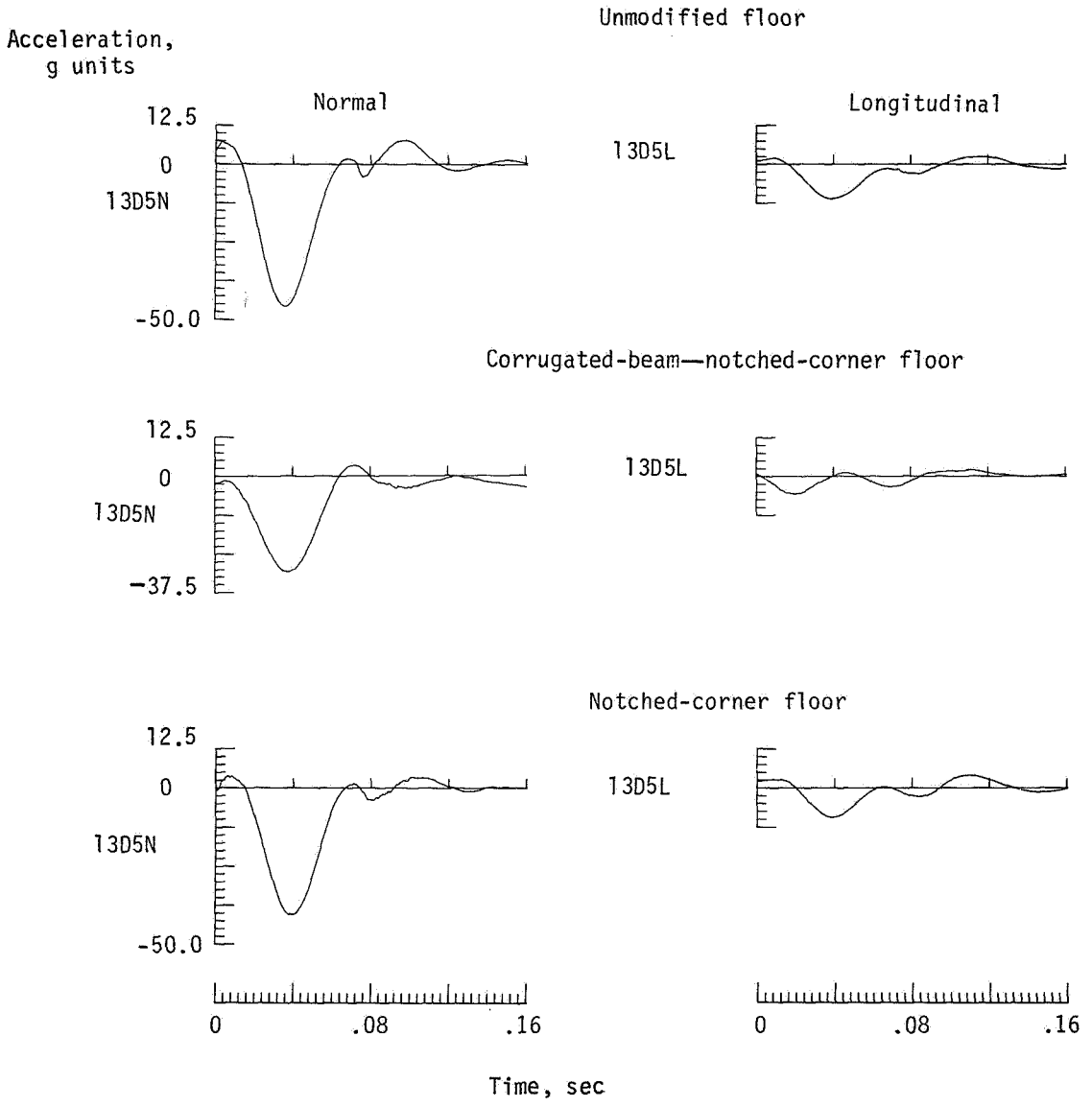

Figure 17. Normal and longitudinal floor accelerations for inboard track of copilot position.

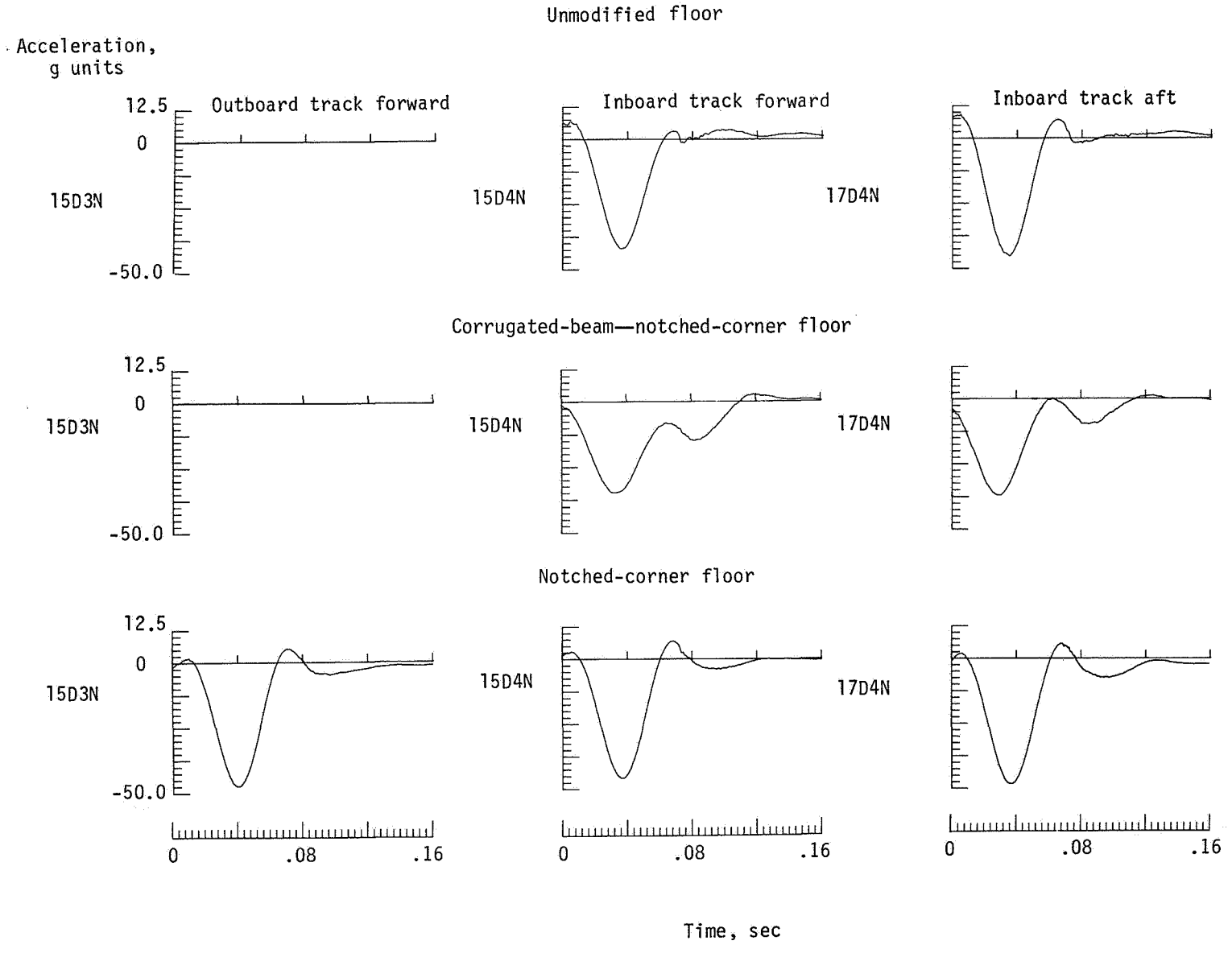

(a) Normal accelerations.

Figure 18. Floor accelerations for first passenger position.

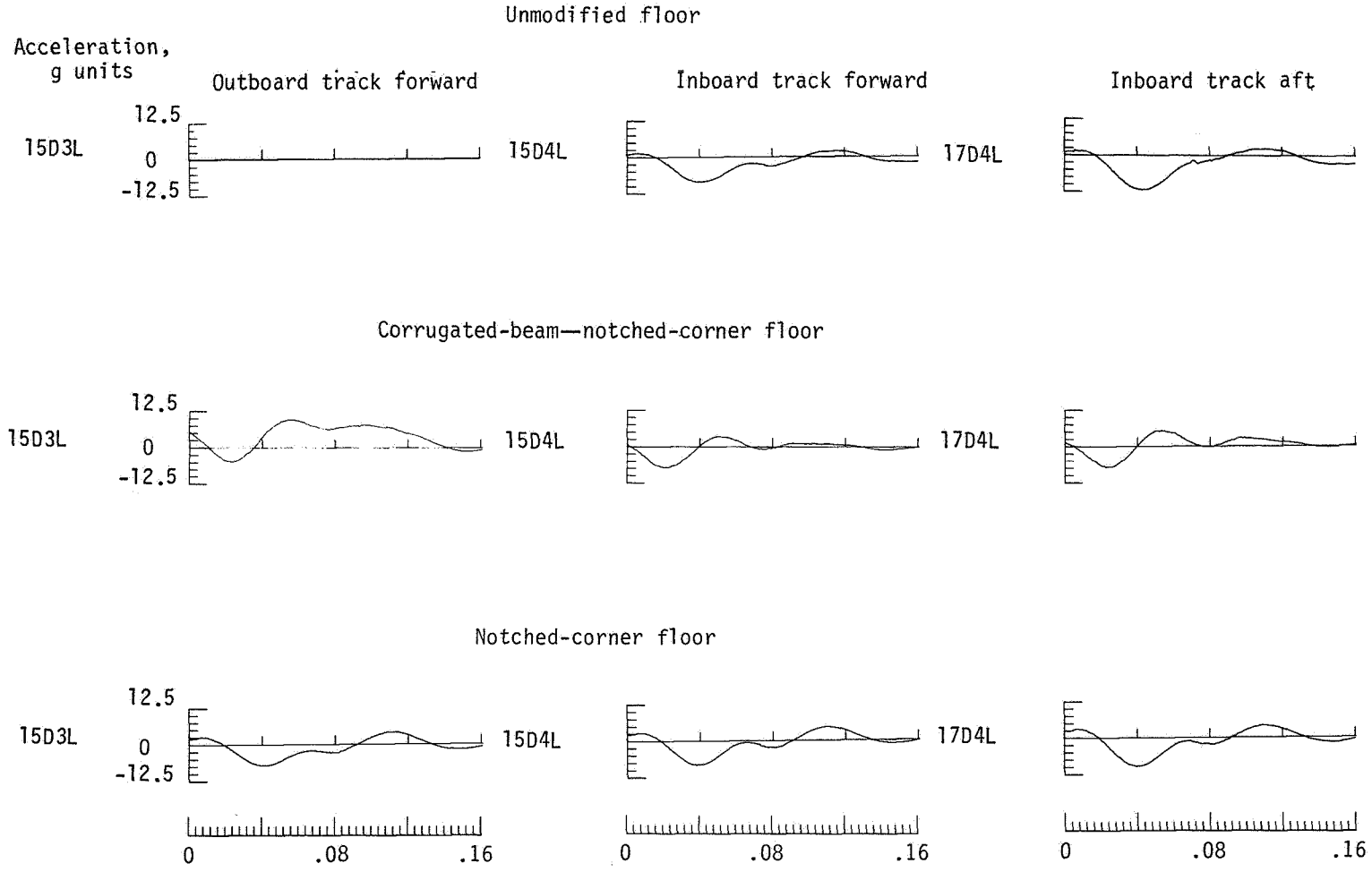

(b) Longitudinal accelerations.

Figure 18. Concluded.

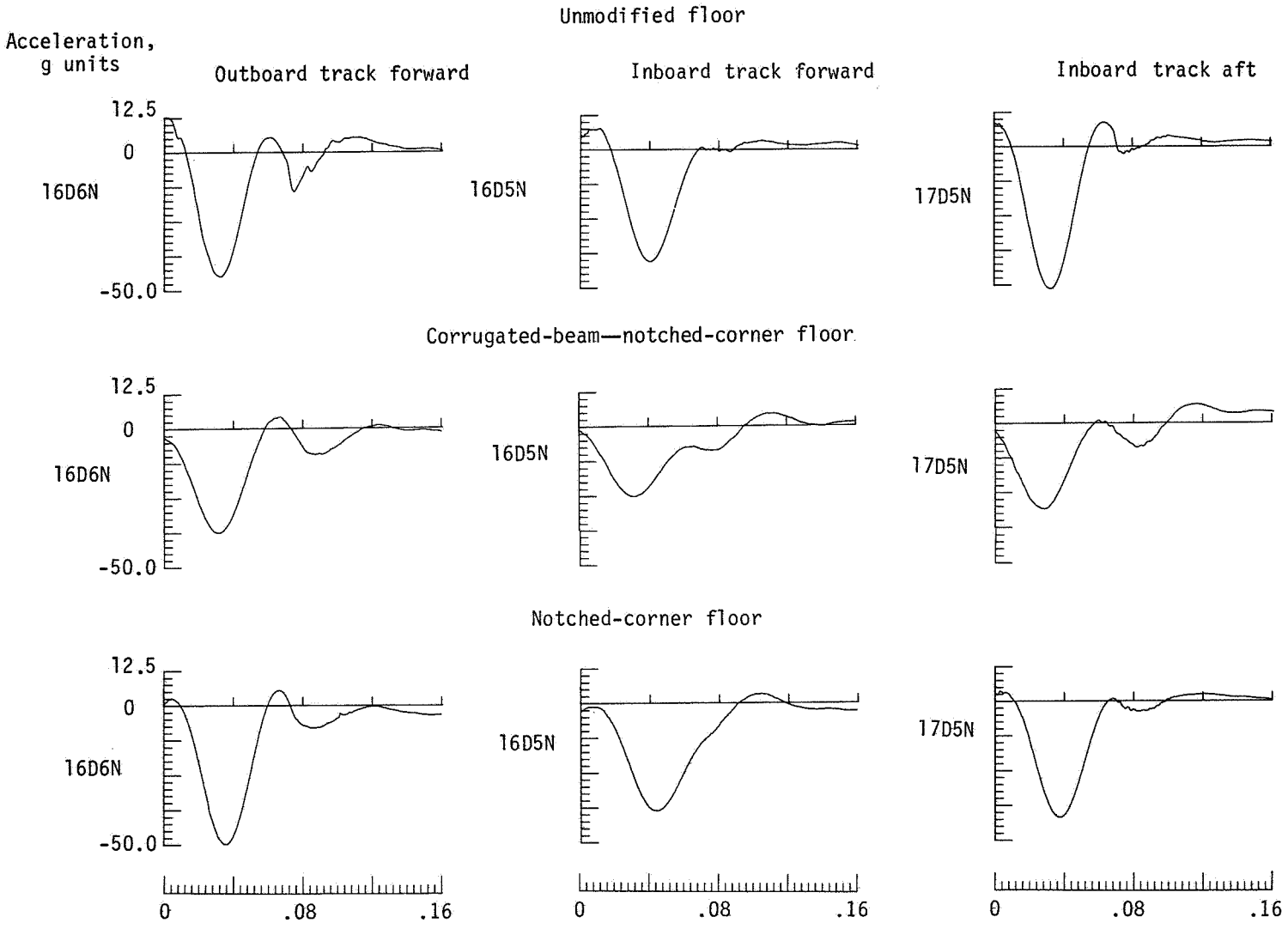

(a) Normal accelerations.

Figure 19. Floor accelerations for second passenger position.

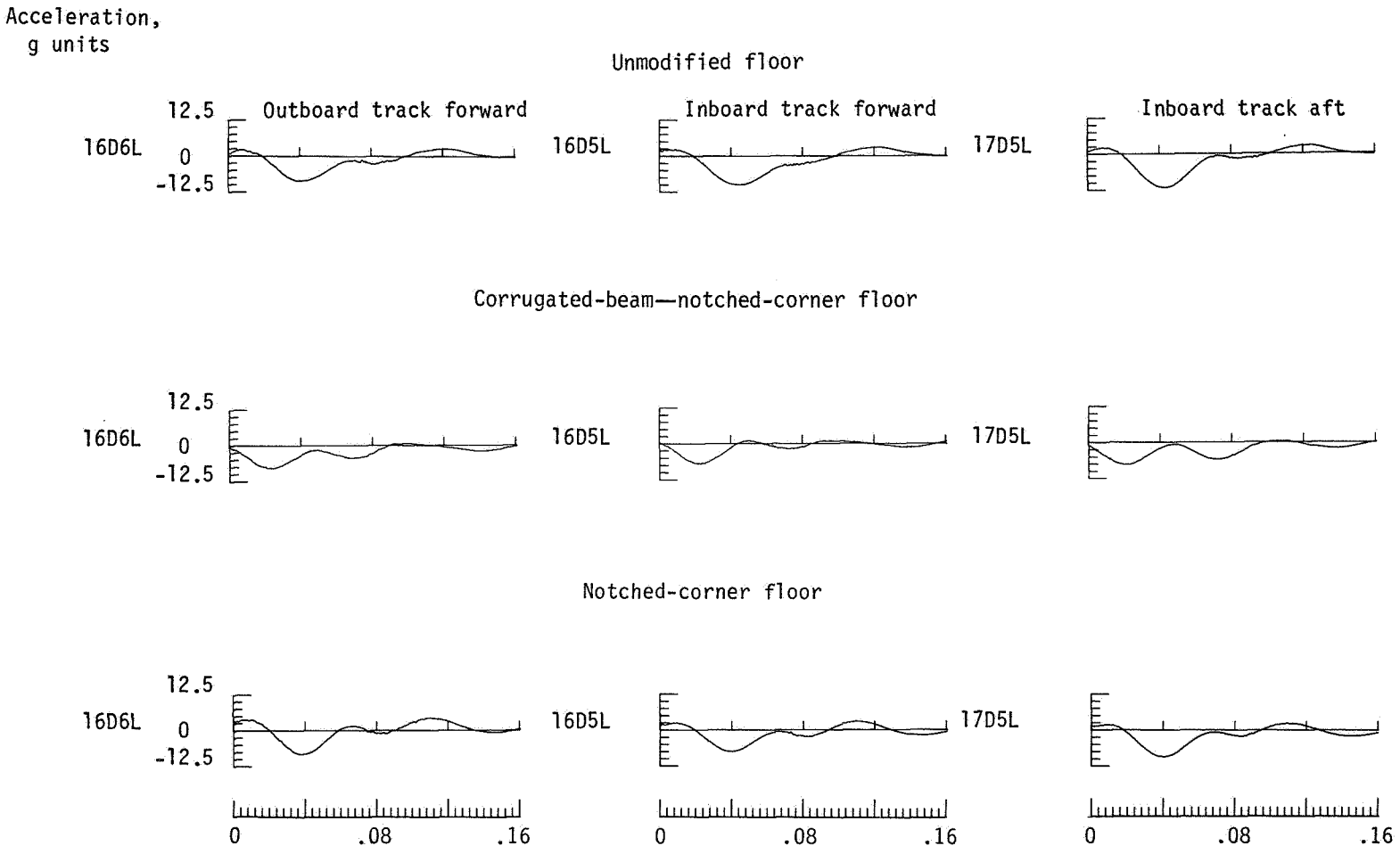

(b) Longitudinal accelerations.

Figure 19. Concluded.

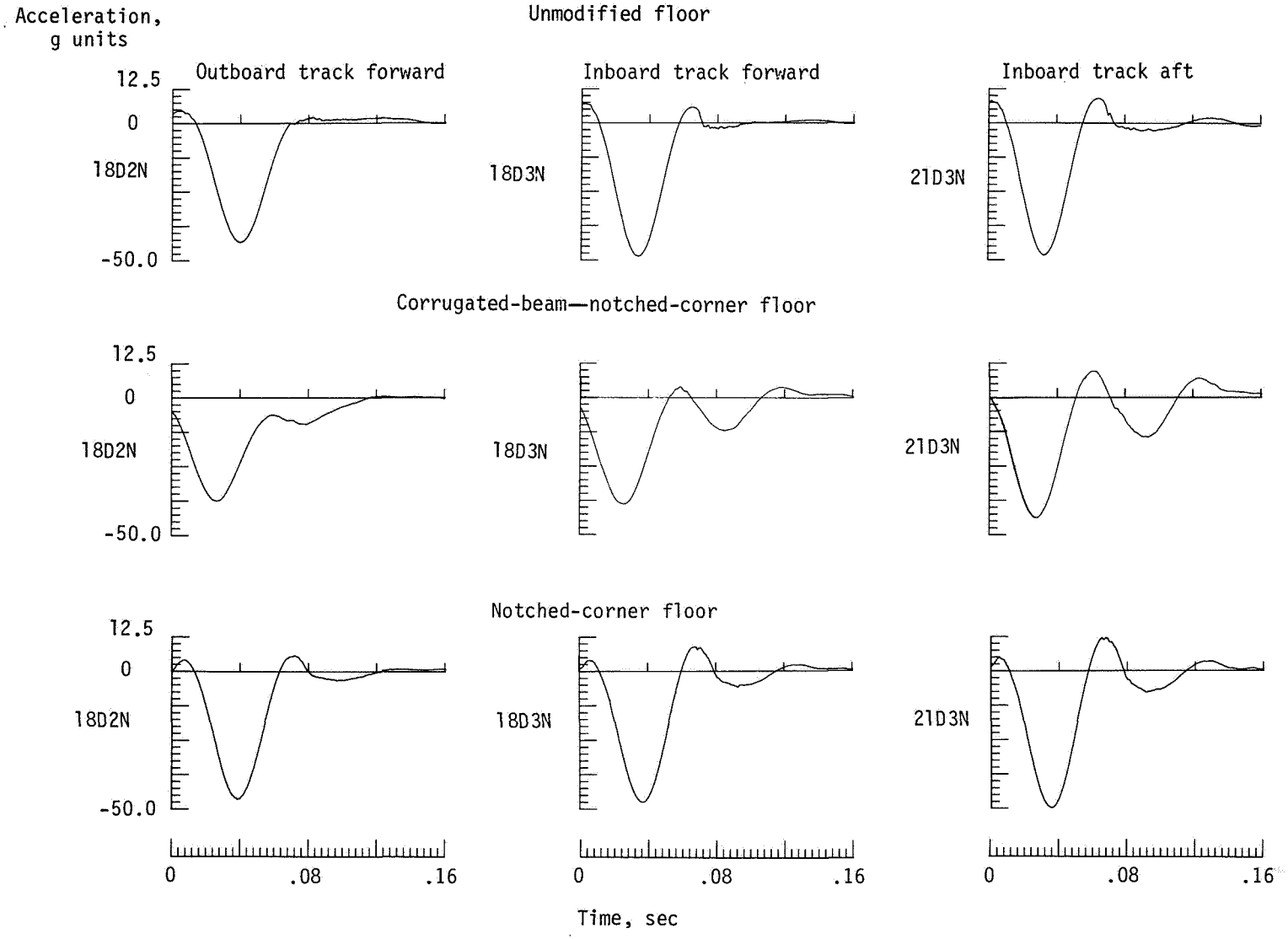

(a) Normal accelerations.

Figure 20. Floor accelerations for third passenger position.

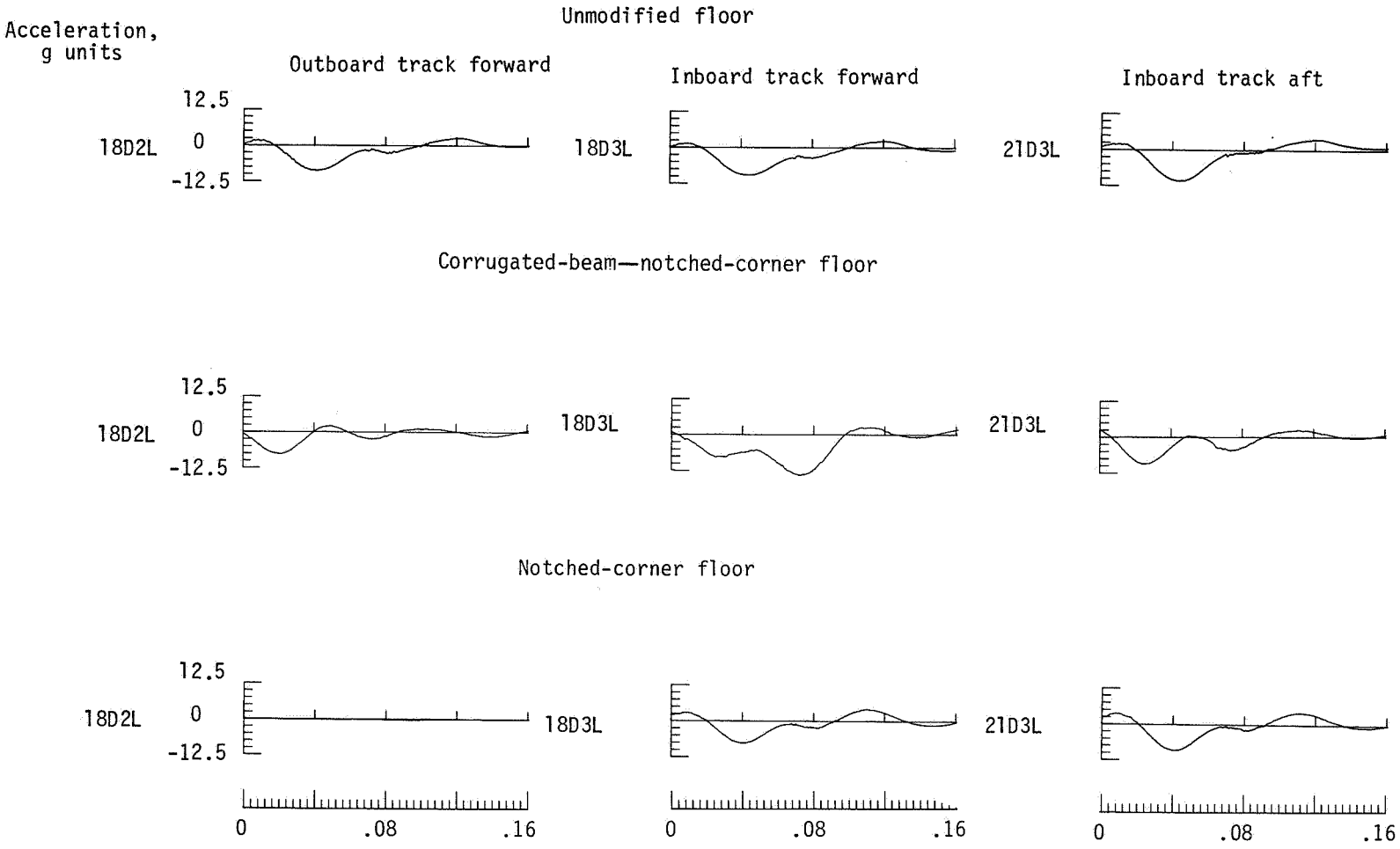

(b) Longitudinal accelerations.

Figure 20. Concluded.

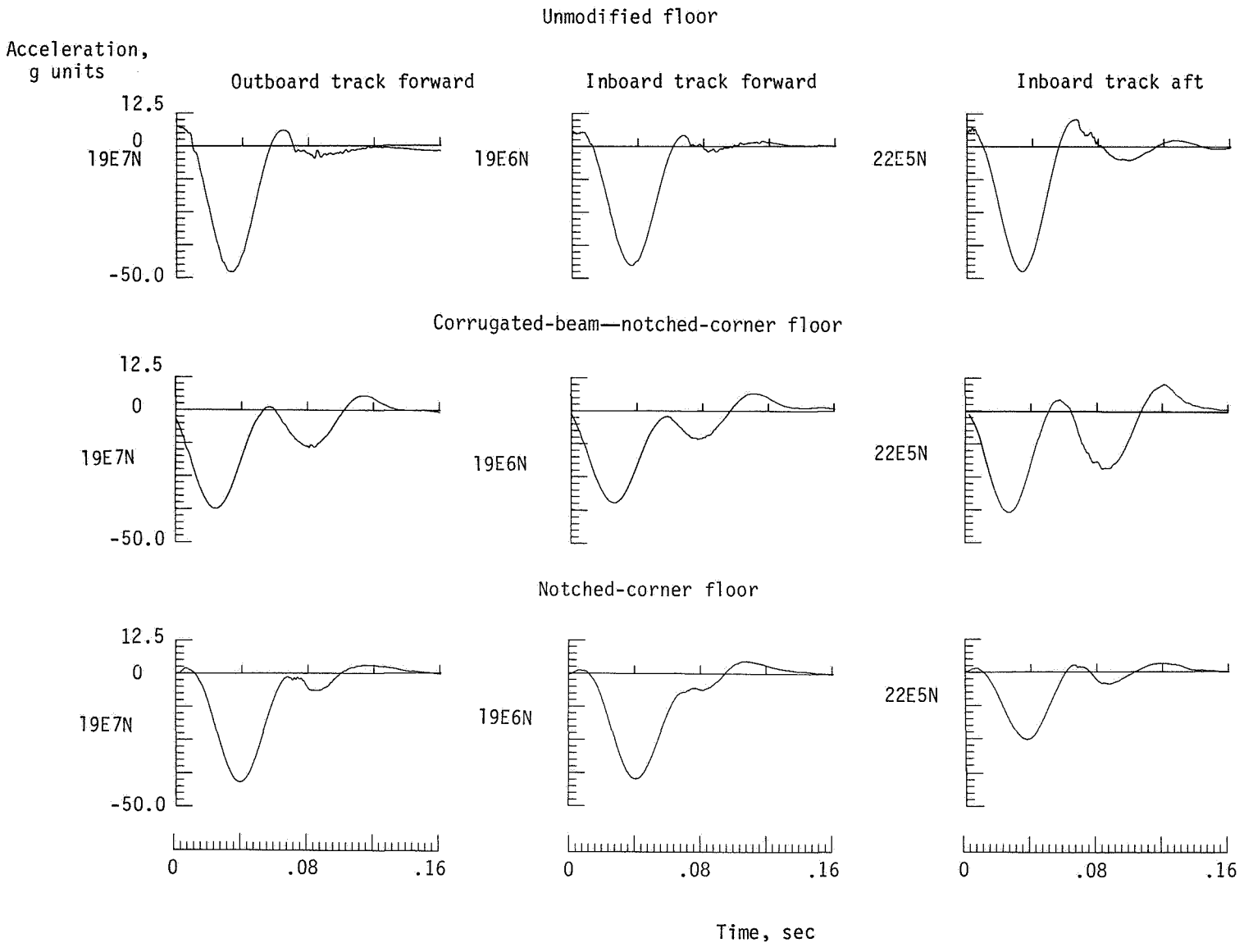

(a) Normal accelerations.

Figure 21. Floor accelerations for fourth passenger position.

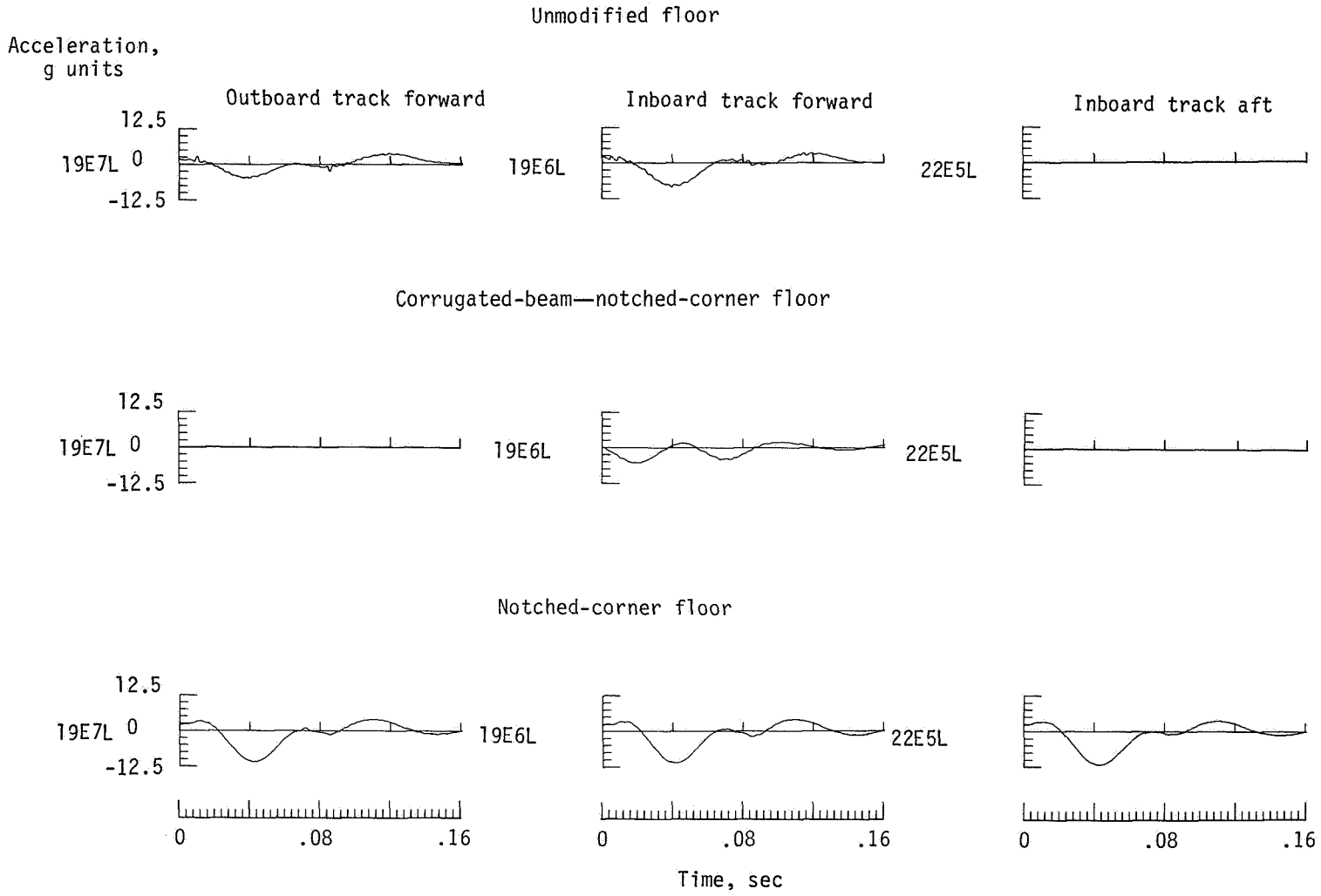

(b) Longitudinal accelerations.

Figure 21. Concluded.

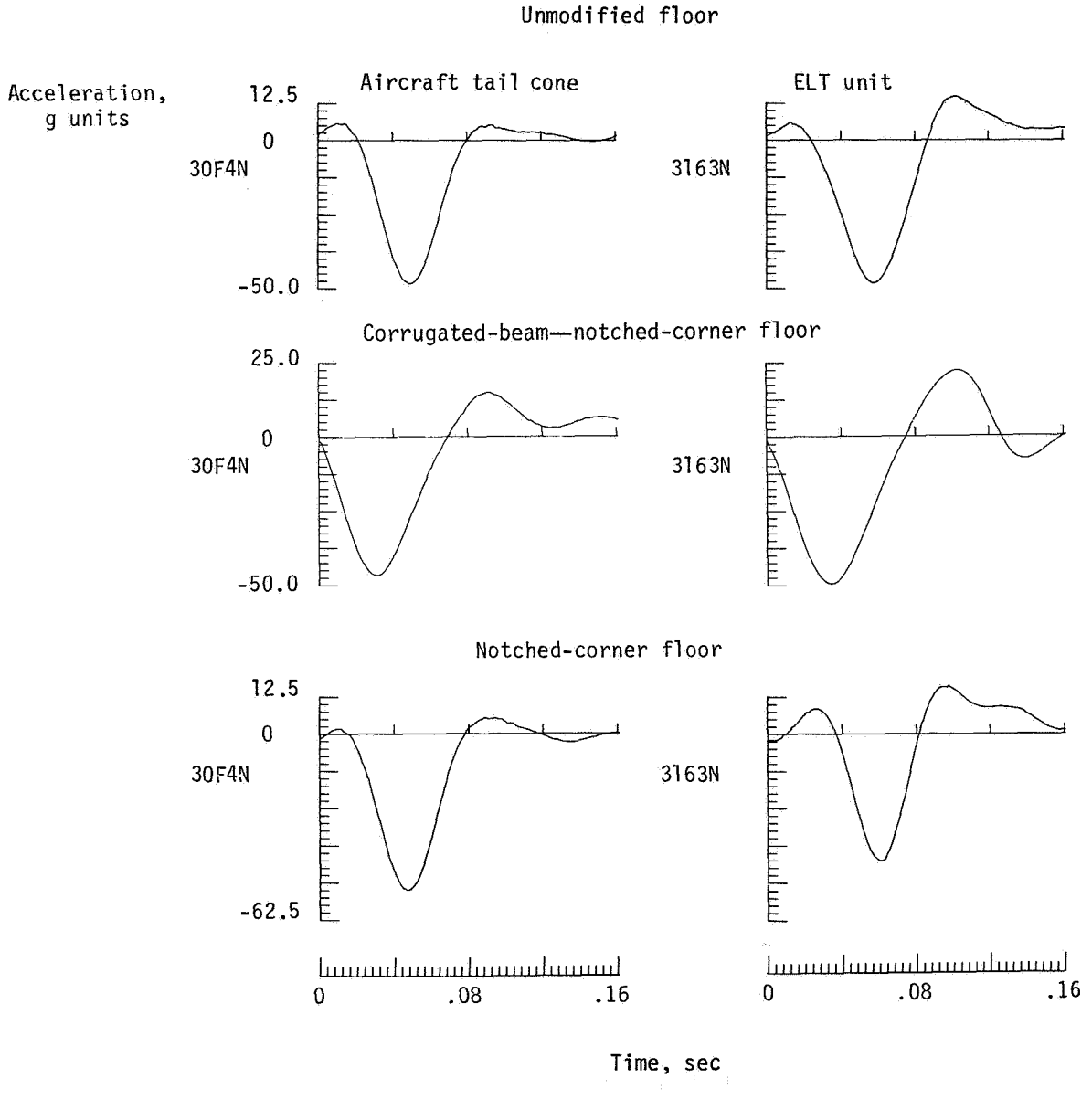

(a) Normal accelerations.

Figure 22. Accelerations in airplane tail cone and on emergency locator transmitter (ELT) unit.

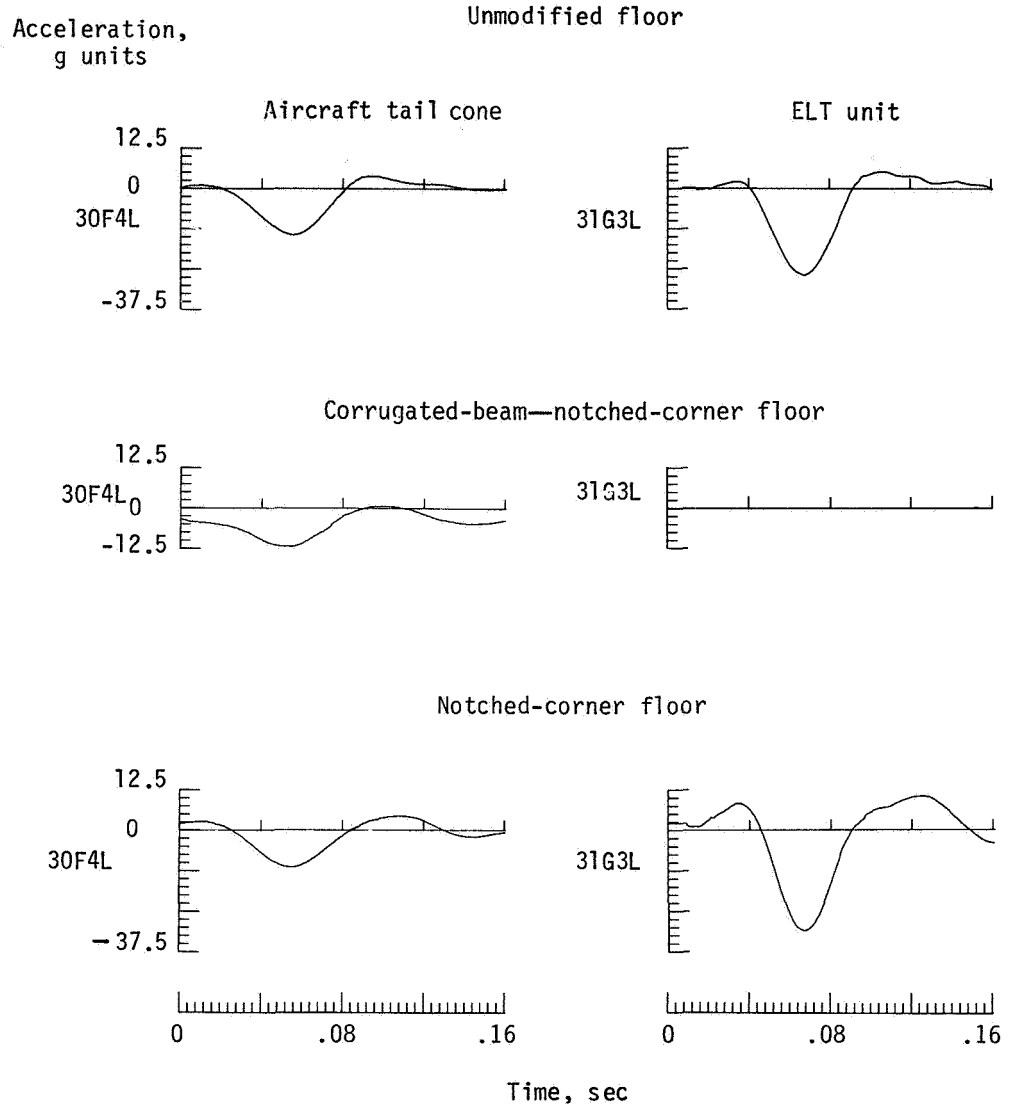

(b) Longitudinal accelerations.

Figure 22. Concluded.

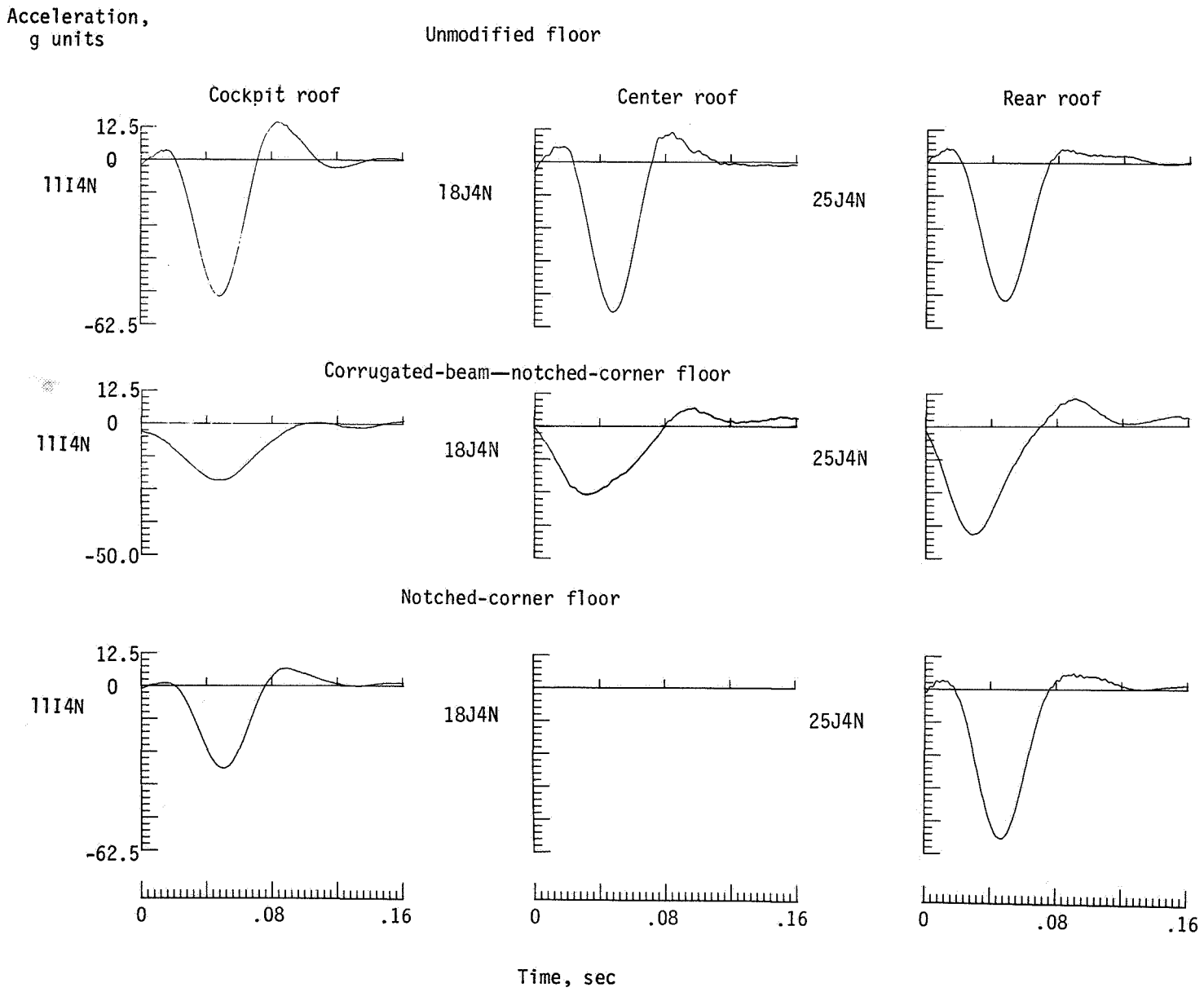

Figure 23. Accelerations for roof of airplane.

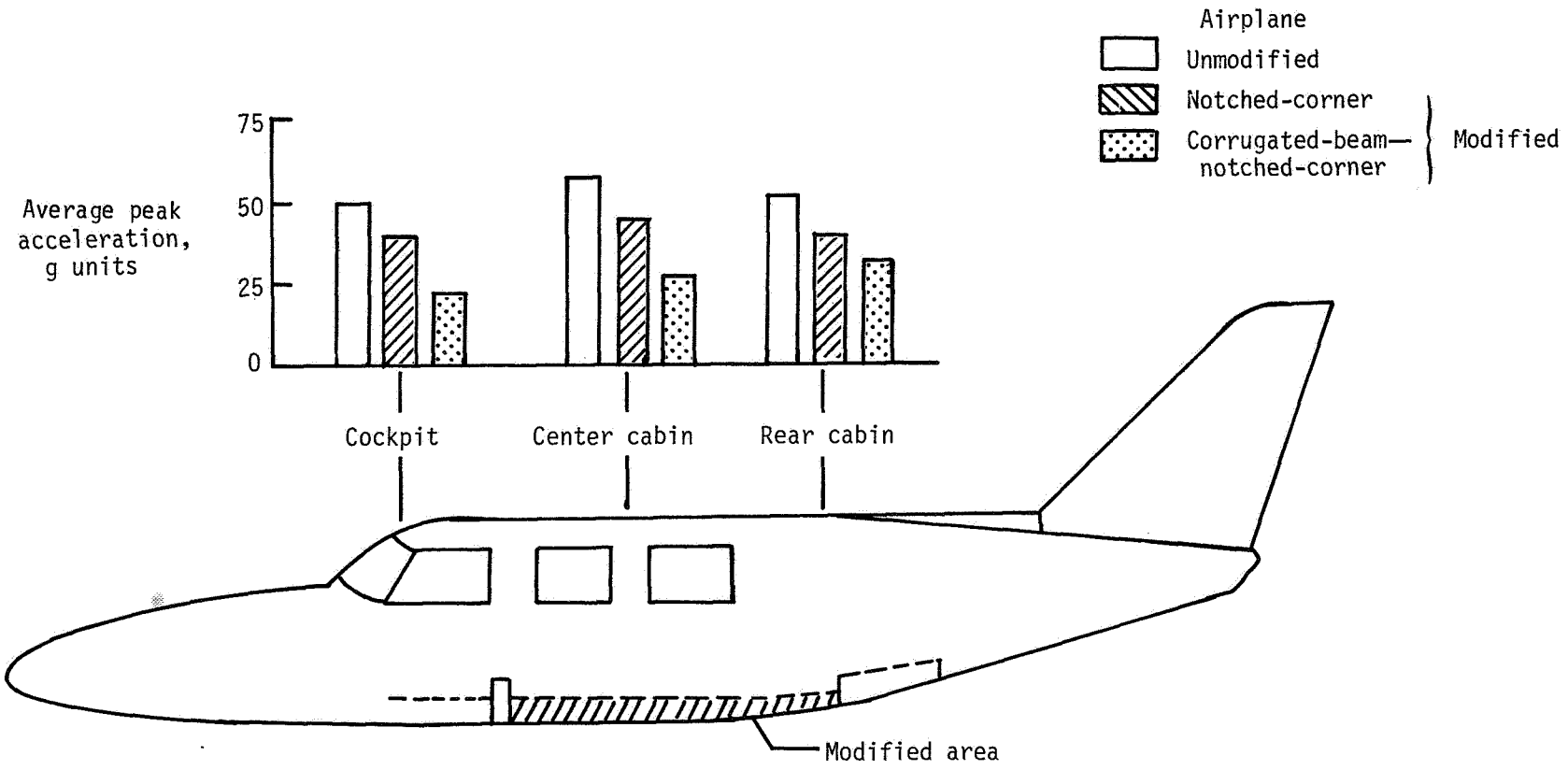

Figure 24. Average peak normal floor accelerations at three airplane locations.

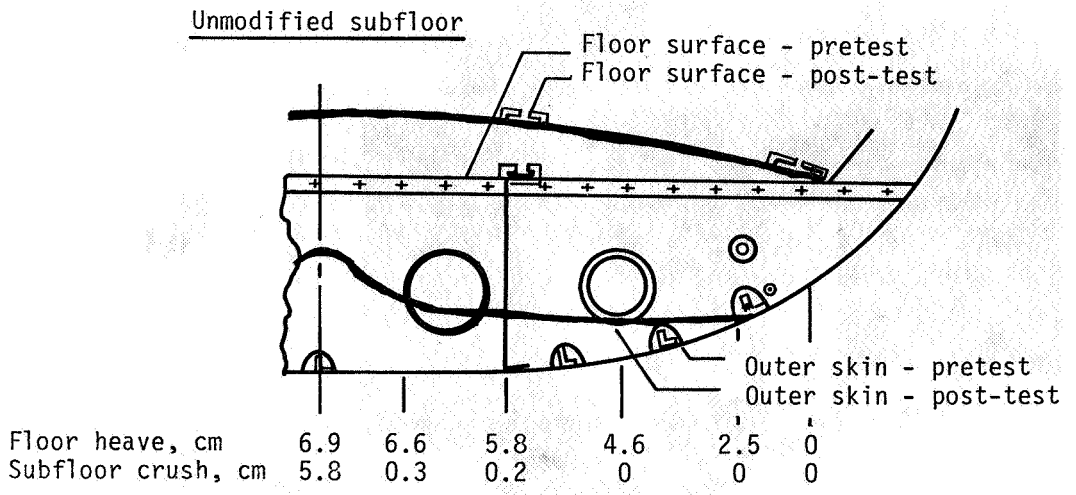

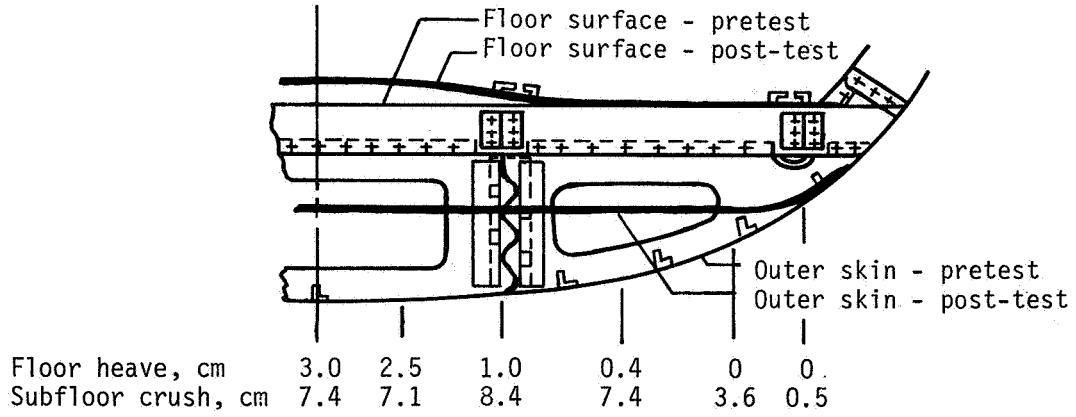

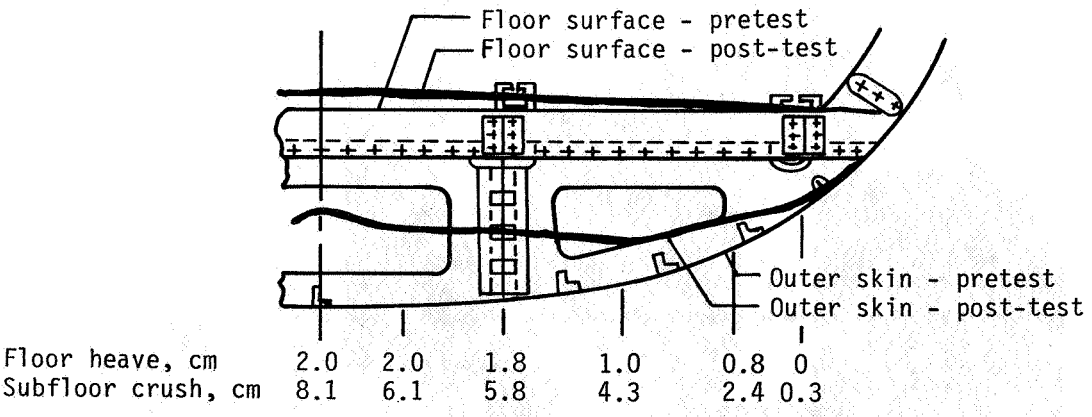

Figure 25. Cross-sections of test airplanes showing floor heave and subfloor crushing at FS 4.83 m.

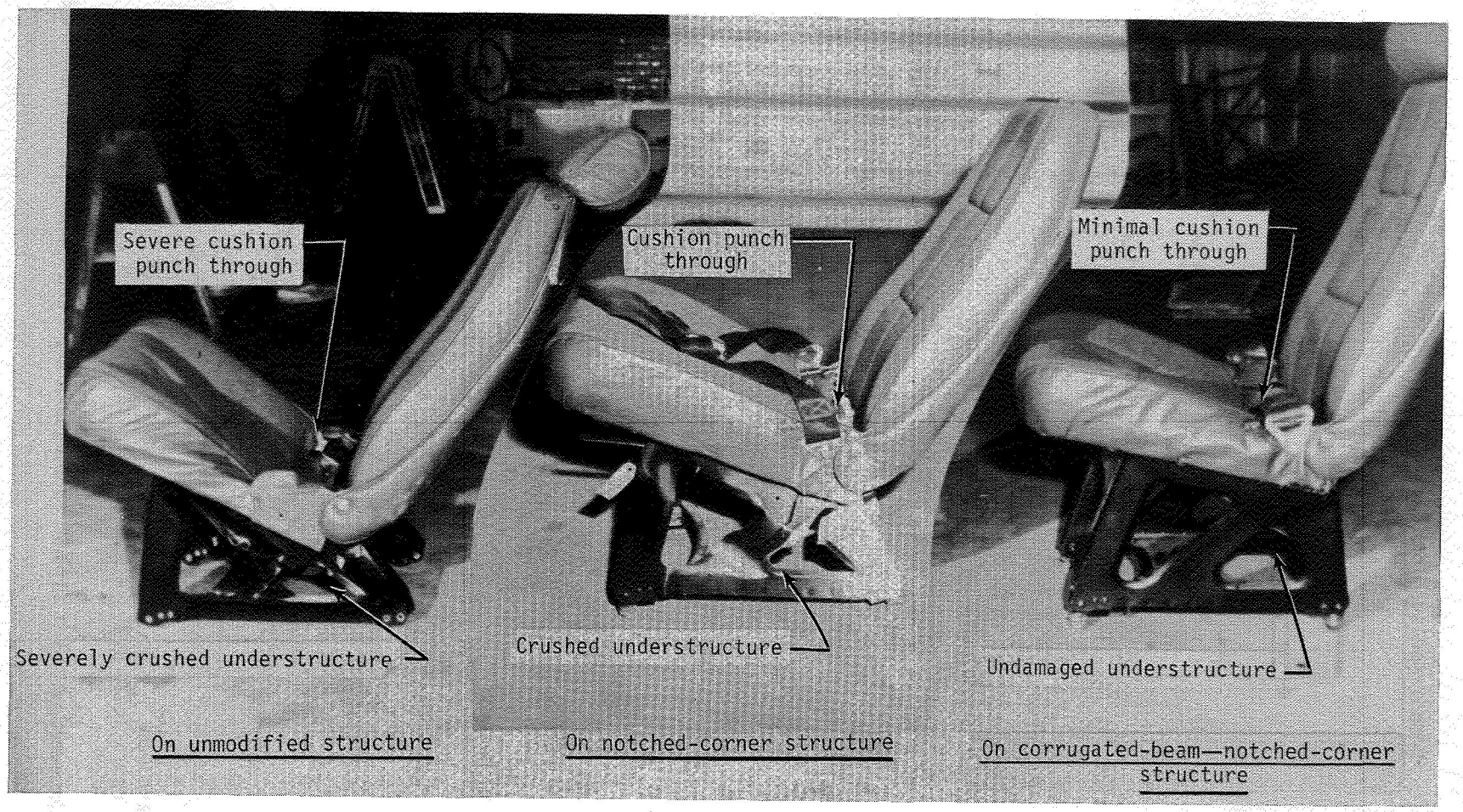

(a) Standard seats.

Figure 26. Crushed standard and load-limiting seats.

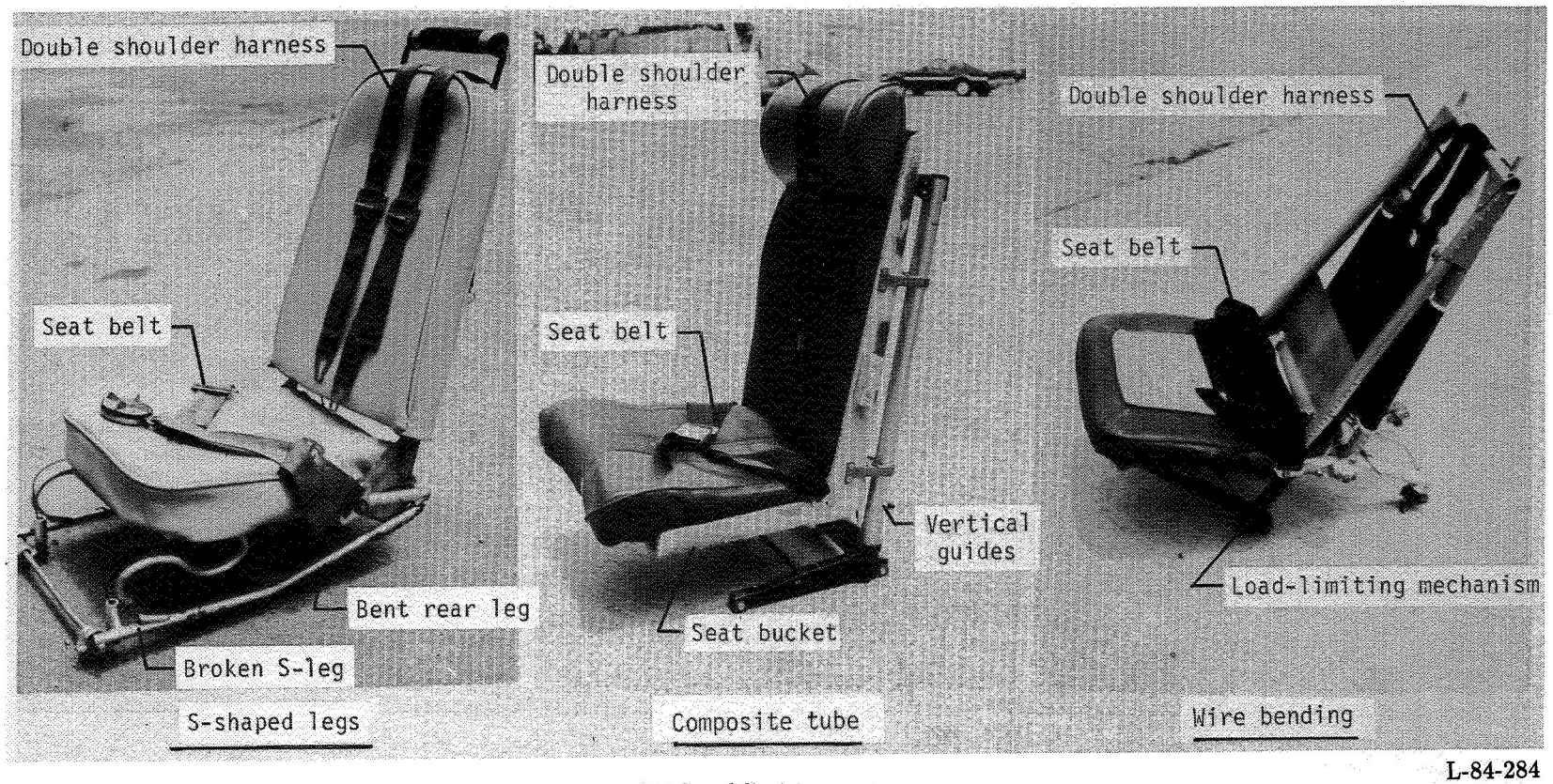

(b) Load-limiting seats.

Figure 26. Concluded.

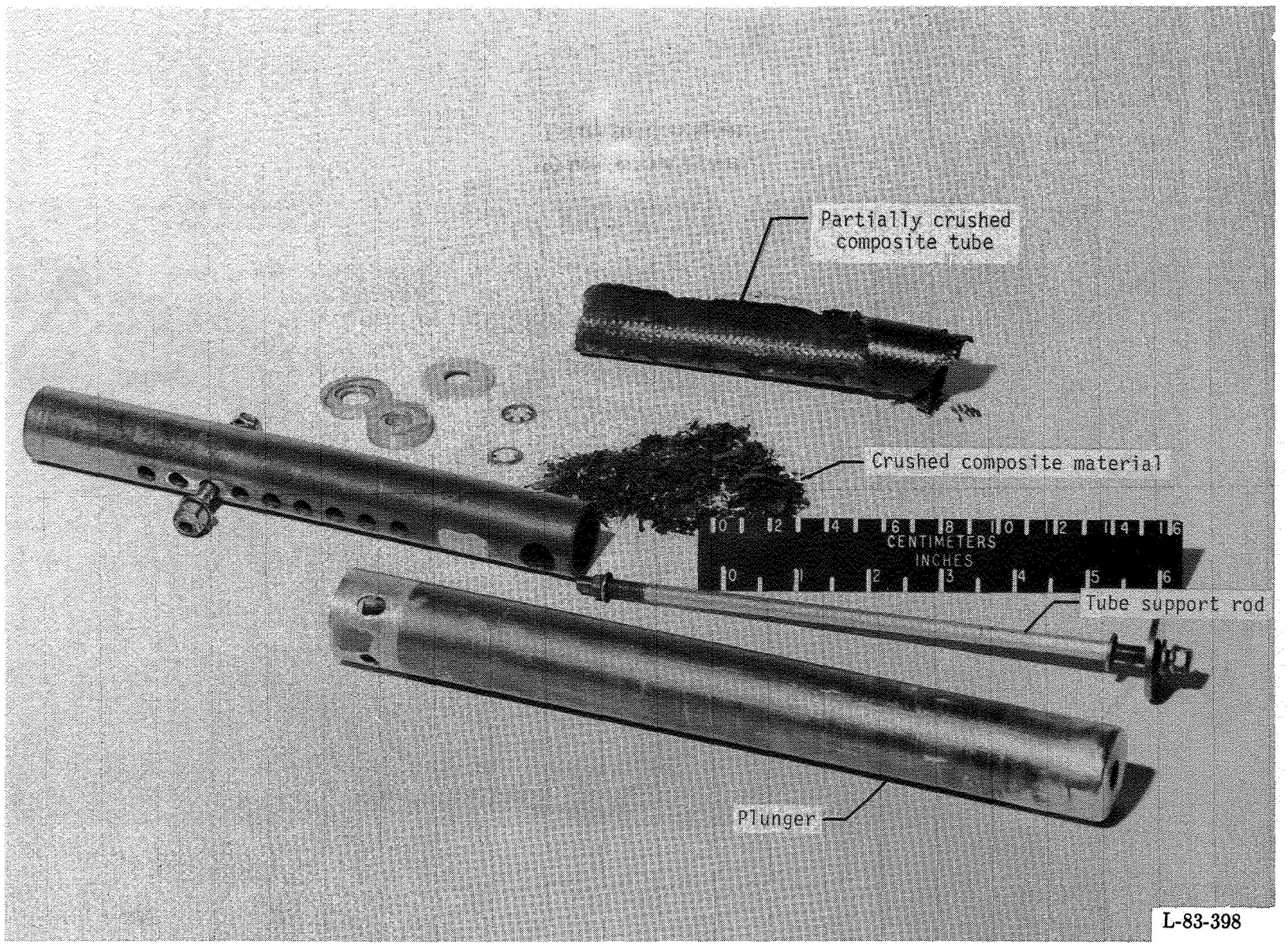

Figure 27. Composite-tube load-limiting mechanism (disassembled) showing partially crushed composite tube.

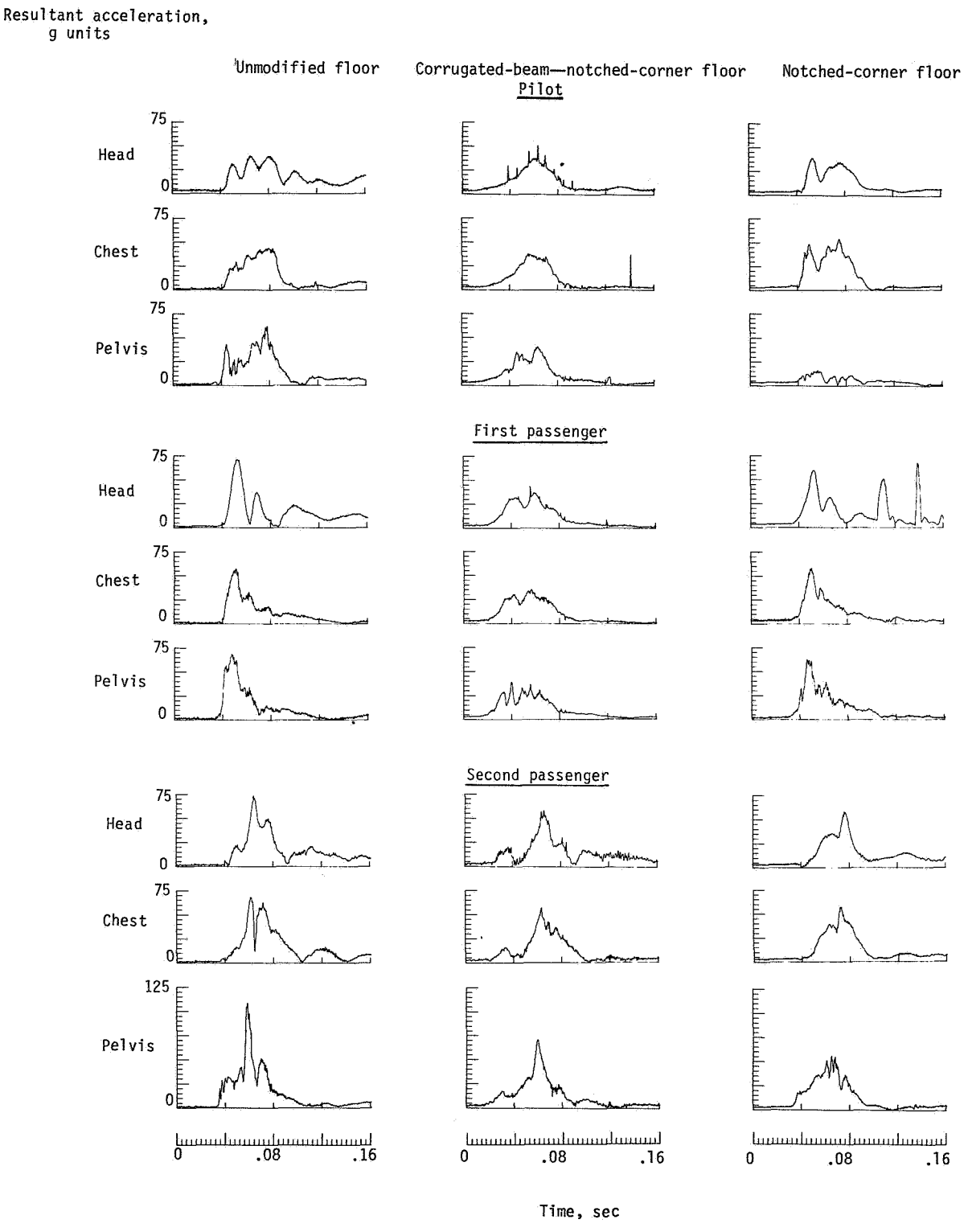

(a) Pilot, first passenger, and second passenger.

Figure 28. Resultant accelerations for anthropomorphic dummies.

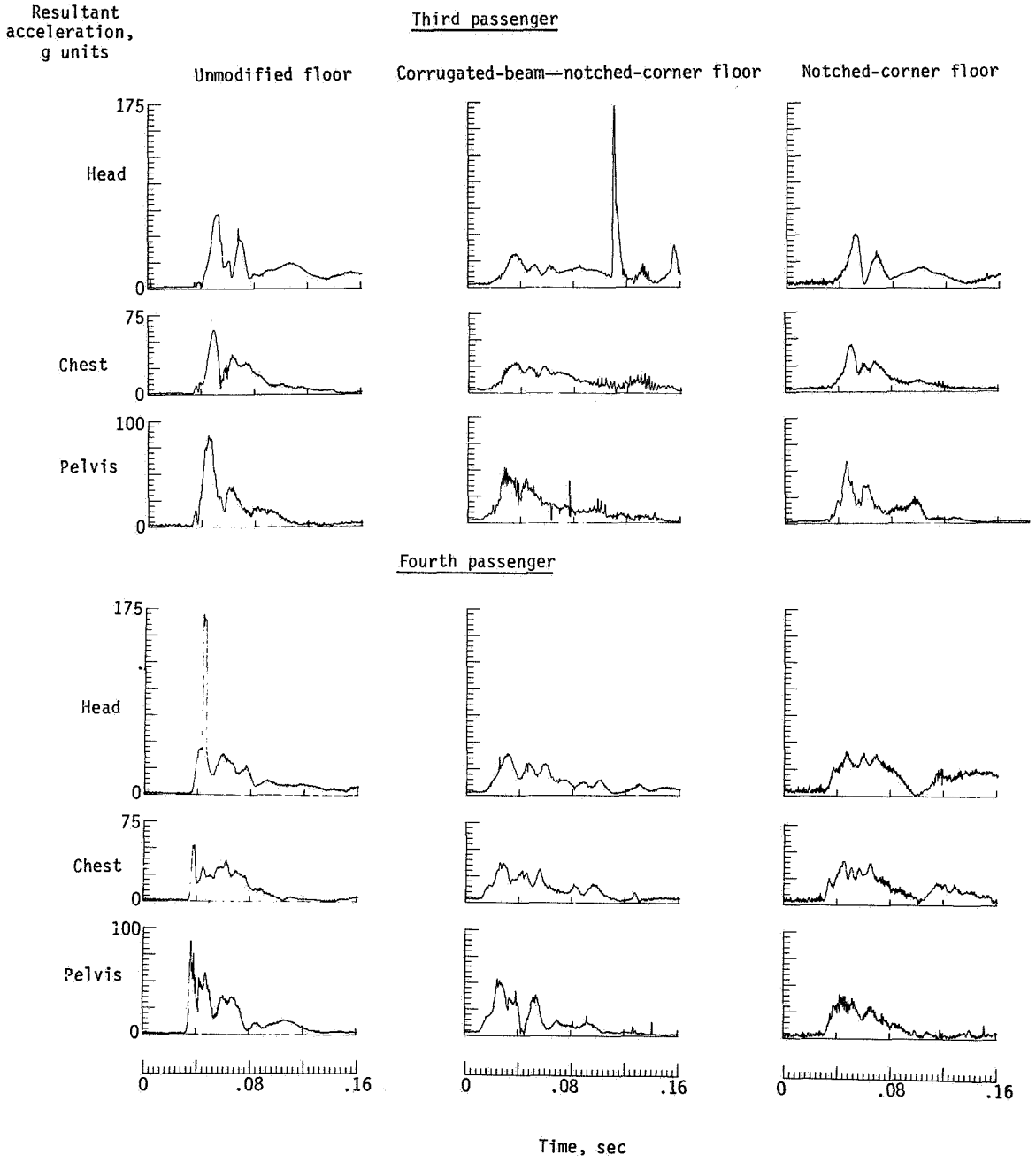

(b) Third and fourth passengers.

Figure 28. Concluded.

1. Report No.	2. Government Accession No.	3. Recipient's Catalog No.
NASA TP-2380		

4. Title and Subtitle	5. Report Date
FULL-SCALE CRASH-TEST EVALUATION OF TWO LOAD-LIMITING SUBFLOORS FOR GENERAL AVIATION AIRFRAMES	December 1984
	6. Performing Organization Code: 505-33-53-09
7. Author(s): Huey D. Carden	8. Performing Organization Report No.: L-15764
9. Performing Organization Name and Address: NASA Langley Research Center, Hampton, VA 23665	10. Work Unit No.
	11. Contract or Grant No.
12. Sponsoring Agency Name and Address: National Aeronautics and Space Administration, Washington, DC 20546	13. Type of Report and Period Covered: Technical Paper
	14. Sponsoring Agency Code

15. Supplementary Notes

16. Abstract

Three six-place, low-wing, twin-engine general aviation airplane test specimens were crash tested at the Langley Impact Dynamics Research Facility under controlled free-flight conditions. One structurally unmodified airplane was the base-line specimen for the test series. The other two airplanes were structurally modified to incorporate load-limiting (energy-absorbing) subfloor concepts into the structure for full-scale crash-test evaluation and for comparison with the unmodified-airplane test results. Typically, the lowest floor accelerations, the lowest anthropomorphic-dummy responses, and the least seat crushing of standard and load-limiting seats occurred in the airplanes modified with load-limiting subfloors, wherein the greatest structural crushing of the subfloor took place. The better performing of the two load-limiting subfloor concepts reduced the peak airplane floor accelerations to $-25g$ to $-30g$ as compared with approximately $-40g$ to $-55g$ for the unmodified airplane structure.

17. Key Words (Suggested by Authors(s))
Airplane crash test
Load-limiting subfloor
Load-limiting seats
Crash damage
General aviation
Impact test
Crash dynamics

18. Distribution Statement
Unclassified—Unlimited

Subject Category 39

19. Security Classif.(of this report)	20. Security Classif.(of this page)	21. No. of Pages	22. Price
Unclassified	Unclassified	59	A04

For sale by the National Technical Information Service, Springfield, Virginia 22161

NASA-Langley, 1984

National Aeronautics and
Space Administration

Washington, D.C.
20546

Official Business
Penalty for Private Use, $300

THIRD-CLASS BULK RATE

Postage and Fees Paid
National Aeronautics and
Space Administration
NASA-451

POSTMASTER: If Undeliverable (Section 158 Postal Manual) Do Not Return